Biosynthesized Metallic Nanoarchitecture for Photocatalytic Degradation of Emerging Organochlorine and Organophosphate Pollutants: A Review

Stephen Sunday Emmanuel,*[c, h] Mustapha Omenesa Idris,[a, d] Christopher Olusola Olawoyin,[e, f] Ademidun Adeola Adesibikan,*[b, c] Abdulbasit A Aliyu,[a, d] and Abdulrahman Itopa Suleiman[g]

[a] School of Chemical Sciences, Universiti Sains Malaysia, 11800 Penang, Malaysia

[b] Department of Chemistry, Faculty of Natural and Agricultural Sciences, University of Pretoria, Private Bag X20, Hatfield 0028, Pretoria, South Africa. E-mail: adesibikana@gmail.com

[c] Department of Industrial Chemistry, Faculty of Physical Sciences, University of Ilorin, P. M. B. 1515, Ilorin, Nigeria. E-mail: stephenemmanuel6011@gmail.com

[d] Department of Pure and Industrial Chemistry, Kogi State University (Prince Abubakar Audu University), P.M.B 1008 Anyigba, Kogi State, Nigeria

[e] Department of Biochemistry, Faculty of Life Sciences, University of Ilorin, P. M. B. 1515, Ilorin, Nigeria

[f] Department of Chemistry and Materials Science, Faculty of Natural Science, Novosibirsk State University, 1 Pirogova St. 630090

[g] Department of Science Laboratory Technology, Kogi State Polytechnic, Lokoja, Nigeria

[h] Department of Chemical Sciences, Faculty of Science, University of Johannesburg, Doornfontein Campus, Corner Nind and Beit Streets, P. O. Box 17011, Johannesburg, 2028, South Africa

Abstract

The use of efficacious and cost-effective pesticides (OP and OC) has undoubtedly proven to be a blessing and a baron because these pesticides are safeguarding the world from food insecurity. Unfortunately, their presence in aquatic bodies brings about an upsurge in water pollution. Amazingly, the photocatalytic degradation approach utilizing biogenic nanoparticles (BNPs) is a trendy state-of-the-art approach and has been established to be a sustainable methodology for the complete mineralization of contaminants into harmless molecules. Thus, this work holistically explores the use of BNPs for photocatalytic degradation of OP and OC. Based on the review, it was found that the least amount of time needed for degradation was less than 5 minutes, while the maximum degradation efficiency was >80 %. The dominant radicals participating in the degradation are ·OH and O_2· and this radical dominance was enhanced by the oxygenated functional groups present in the biogenic entities employed for the biosynthesis of BNPs. The photocatalytic degradation data fits the pseudo-first-order and Langmuir isotherm models ($R^2 > 0.9$), which indicates that the main adsorption mechanisms involved during electron-hole pair formation and photocatalytic degradation are physisorption and monolayer at the surface of the BNPs. BNPs can sustain a >80 % degradation efficiency for approximately 5 cycles and are reusable for up to 8 cycles. It was also revealed that plants constitute 80 % of the engaged biogenic entities for BNP synthesis. Ultimately, this work offers novel avenues and future research hotspots that might accelerate the use of BNPs for sustainable agricultural and wastewater management practices.

Graphical Abstract

This review study shows that biogenic nanoparticles and photocatalytic degradation are game changers in the field of environmental pollution remediation for the photocatalytic degradation of organochlorine and organophosphorus pollutants in aquatic environments as the various reported green nanoparticles can be reused up to 8 times with >90 % degradation efficiency at the last regeneration cycle in most cases.

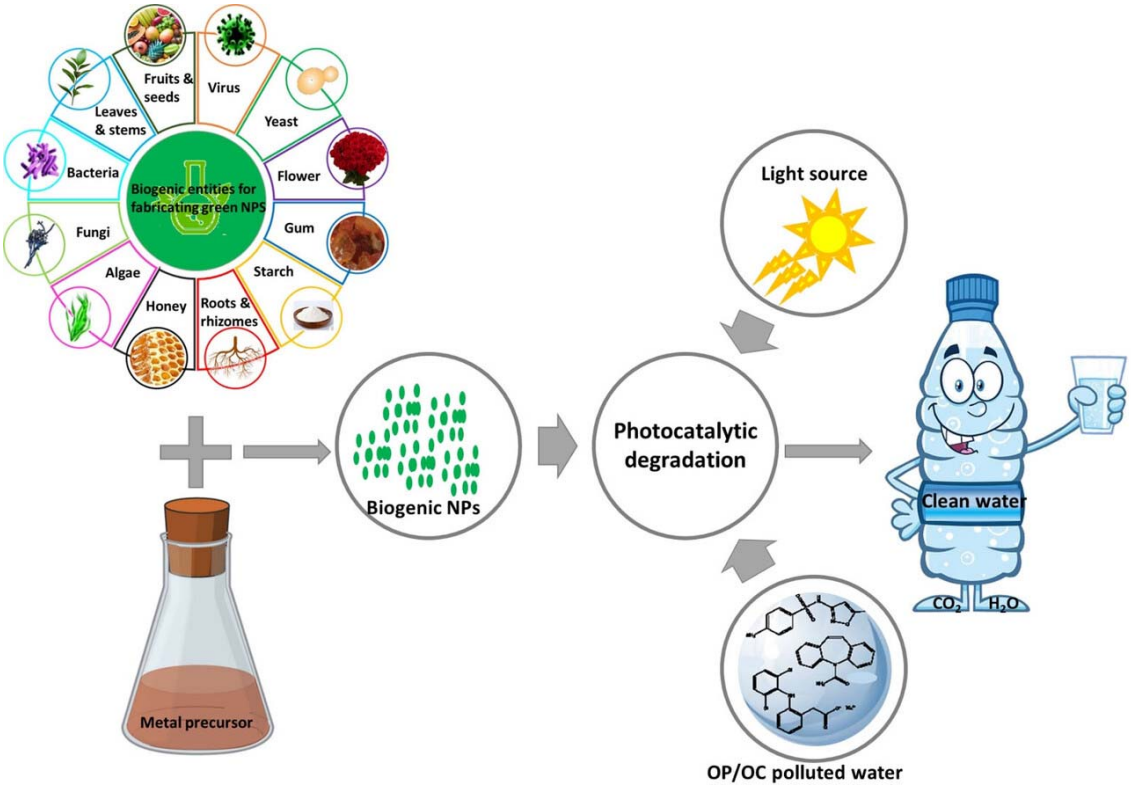

1. Introduction

Pesticide residues are disseminated into the environment due to rapid industrialization and their widespread application in agricultural practices. Pesticides are of vital importance in modern agriculture because they protect crops against pests and diseases.[1] The increased usage of these compounds, however, has generated concerns about their influence on human health. Pesticide use has risen, resulting in greater exposure to these substances for farmers, agricultural workers, and the public at large during the last few decades.[2] It has prompted considerable concerns about the possible risks of these compounds and their effects on human well-being (Figure 1). The harmful effects of many pesticides on people's health have been widely recognized and studied.[3] Organochlorines and organophosphates, for example, accumulate acetylcholine in the human central nervous system, causing significant brain disorders.[4] Organochlorines and organophosphates are highly hazardous pesticides with many-year half-lives. Although several governments worldwide have passed regulations prohibiting these pesticides, a wide range of pesticides are still present in coastal environments.[5] Their removal has become necessary due to their high persistence, toxicity, and propensity for bioaccumulation. Organochlorine pesticides are chlorinated hydrocarbons, whereas organophosphates are primarily amides, esters, or thiol derivatives of phosphoric-based acids.

These are endocrine disruptor chemicals that cause severe chronic and developmental toxicity, resulting in about 1 million poisoning cases every year.[6, 7]

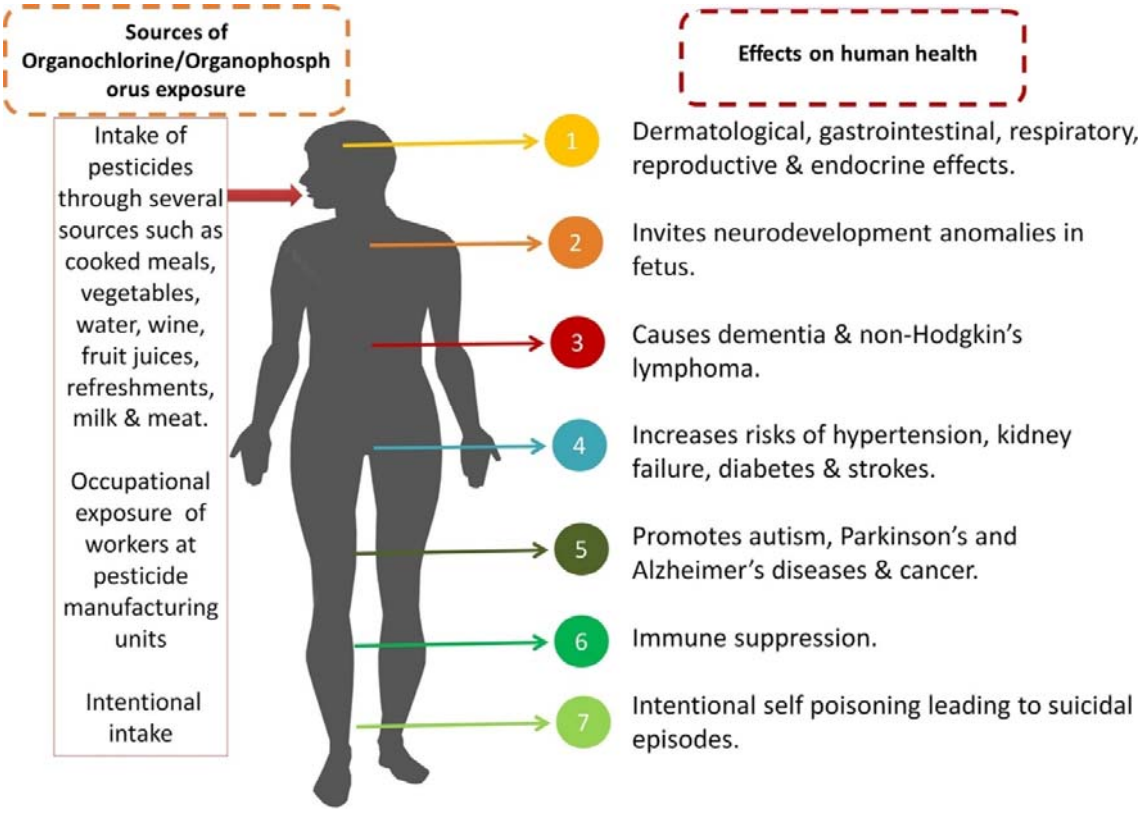

Figure 1. Exposure route and health impacts of OC/OP pesticide in humans.[8]

Many attempts have therefore been made to eliminate these dangerous toxicants from environmental matrices. These efforts have made use of a range of removal techniques, including adsorption, chemical precipitation, membrane separation, bio-electrochemical devices, advanced oxidation processes, and photocatalytic degradation.[9-18] The photocatalytic approach has rekindled the interest of scientists as an alternate strategy for the complete mineralization of pesticides. Solar energy, UV, as well as visible light, are used to irradiate nanosemiconductors, leading to the formation of a variety of radicals, particularly hydroxide and superoxide radicals, that are necessary for photodegradation.[19] When the pollutant is adsorbed on the surface of the nano-photocatalyst, photocatalytic activity can be enhanced.[20] When selecting an appropriate material for photocatalytic degradation, photo-activity, chemical, and photo stability, and the band gap of the photocatalyst are all factors to be taken into account.[12, 21] A wide range of nanoparticles have been effectively used to mitigate the environmental effects of pesticides.[22, 23] Metallic nanoparticles' unique shapes and great catalytic potential have recently been utilized. Because of their huge surface area, they are good heterogeneous catalysts. Furthermore, these nanostructure catalysts may be recovered and recycled from the reaction mixture with ease. However, the aggregation and toxicity of these metallic nanoparticles remain major concerns.[24, 25] The eco-friendly biosynthetic nanoparticles derived from plants or microbes are emerging as the most suitable material for photocatalytic degradation.[12, 13, 15, 26]

Meanwhile, based on the exhaustive literature survey done by the authors, nanomaterials for the degradation of various pesticide families have received few reviews. The main direction of these earlier review studies has been compared in Table 1 with the novelty and main objectives of this present review paper. Notably, some gaps and observations were noticed. Firstly, certain works concentrate only on the use of metal oxide NPs with special emphasis on non-biogenic metal oxide NPs for the degradation of pesticides in general. For instance, Vaya and Surolia[27] have written a review mainly focusing on non-biogenic semiconductor-based for pesticide degradation and mineralization in aqueous environments. de Oliveira's team[23] study primarily reviewed the combined effect involving plasmonic and semiconductor non-biogenic NPs in degrading pesticides under photo influence, while Shanaah et al[28] primarily focused only on the utilization of non-biogenic metal oxides and their composites for both photocatalytic degradation and adsorptive removal of pesticides. Secondly, some reviews extended the focus of the study to the degradation of only one type of organophosphorus using metal oxide NPs. For example, Ahmad's team[29] work briefly discusses the mechanism of non-biogenic metal oxide NPs for photocatalytic degradation of only diazinon. Thirdly, some reviews are solely written on one particular metal oxide for the photocatalytic degradation of pesticides. Khan and Pathak's[30] work focused only on zinc oxide NPs for the photocatalytic degradation of pesticides, and this is in parallel to another review paper[31] that primarily focuses on the use of only titanium dioxide nanoparticles for the photocatalytic degradation of pesticides. Lastly, there exists a book chapter[32] that focuses on biofabricated nanomaterials for sequestration of all kinds of pesticides using all kinds of techniques, including adsorption, ultrasonication, photo, and enzymatic degradation, without critically and comprehensively analyzing the pesticide elimination efficiency and without looking at the mechanism, regenerability, and recyclability of the biofabricated nanomaterials at all. The key novelty of this present review work compared to the previously reported work highlighted in Table 1 is that it is the first review to provide comprehensive recent advances in the direction of biogenic NPs as photocatalysts towards the photocatalytic degradation of organochlorine and organophosphorus contaminants in water systems. An overview of OP and OC fate and sources in aquatic environments was first conducted to set the tone for why the review is important. As part of the objectives to buttress the novelty of the study, the review article seeks to pragmatically examine the role of different biogenic nanoparticles in the photocatalytic degradation of organochlorine and organophosphate pesticides that are released into the environment. The potential of eco-friendly biosynthesized nanoparticles such as silver NPs (Ag NPs), gold NPs (Au NPs), zinc oxide NPs (ZnO NPs), copper oxide NPs (CuO NPs), and titanium dioxide NPs (TiO_2 NPs) in fighting the deadly effects of organochlorine and organophosphates to maintain an environment that is safe and healthy is also discussed holistically by objectively analyzing the efficiency of these biogenic NPs. Furthermore, a detailed overview of the photocatalytic degradation mechanisms and pathways of OP and OC was also presented to help the readers understanding. Details of adsorption that occur during the photocatalytic degradation of OP and OC using BNPs are revealed using the kinetics and isotherm models to corroborate the explanation of the photocatalytic degradation mechanism. Another unique objective of this present study was to address the economic feasibility doubt of biogenic NPs in the degradation of OC and OP by empirically discoursing and evaluating the regenerability and reusability of expended BNPs, which has not been covered in any single review paper on this subject. In the end, we also offer insightful knowledge gaps from various challenges identified that can help researchers identify potential gaps and also provide suggestions and outlooks for the future to further this area of study.

Table 1. Comparison between this present review study novelty and earlier reviews related to the degradation or elimination of pesticides using various nanomaterials.

Year	The key novelty of the review	Reference (Author)
2021	It focuses on examining the catalytic effectiveness of non-biogenic heterojunctions that are used to degrade pesticides in UV or visible light.	[9]
2019	The work examines the impact of several gamma radiation doses on the degradation of only four organophosphate compounds: dimethoate, chlorfenvinphos, profenofos, and diazinon.	[33]
2020	With a primary focus on non-biogenic semiconductor-based photocatalytic reactions, the paper explains many methods of pesticide degradation and mineralization in aqueous environments.	[27]
2021	Focused only on the function of non-biogenic nanocatalysts in the general treatment of OC compounds	[34]
2017	Mainly focused only on current methods for using non-biogenic NPs to remove and degrade organochlorine insecticides	[35]
2024	The book chapter focused on biofabricated nanomaterials for the sequestration of all kinds of pesticides using adsorption, ultrasonication, photo, and enzymatic degradation without looking at the mechanism, regenerability, or recyclability.	[32]
2021	The study conducted a thorough evaluation of all the research publications on the use of only titanium dioxide nanoparticles in the photocatalytic degradation of pesticides.	[31]
2020	Focus only on zinc oxide NPs for photocatalytic degradation of pesticides	[30]
2022	Largely focused on the performance of non-biogenic nanomaterials for pesticide remediation.	[36]
2022	Focused on the application of non-biogenic nanocomposites in the adsorption and photocatalytic degradation of pesticides.	[37]
2022	Primarily reviewed the combined effect involving non-biogenic plasmonic and semiconductors NPs in degrading pesticides under photo influence	[23]
2021	Focused on the application of non-biogenic nanocomposites for the removal of various pesticides via adsorption and photocatalytic degradation	[38]
2022	The work briefly discusses the mechanism of non-biogenic metal oxide NPs for photocatalytic degradation of only diazinon	[29]
2023	Primarily focused only on the utilization of non-biogenic metal oxides and their composites for photocatalytic degradation and the adsorptive removal of pesticides	[28]
2022	Reviewed recent advances in the oxidative degradation of pesticides, with a main focus on the application of non-biogenic semi-conductive nanomaterials	[39]
2024	Pragmatically focuses on providing recent advances in the direction of biogenic metallic NPs, metal oxide NPs, and their nanocomposites as photocatalysts towards the photocatalytic degradation of organochlorine and organophosphorus contaminants in water systems by critically analyzing their efficiency. Used kinetics and isotherm models to explain the adsorption that occurs during the photocatalytic degradation of OP and OC using biogenic NPs to corroborate the general photocatalytic degradation mechanism. Underscore the economic feasibility doubt of biogenic NPs in the degradation of OC and OP by empirically discoursing and evaluating the regenerability and reusability of expended biogenic NPs.	Present study

2. Review Methodology

Figure 2 depicts the general screening procedures and the flow of choosing pertinent material. The international databases specified in Figure 2 were searched for peer-reviewed literature from 2004 to 2024 in order to gather pertinent data from publications until March 2024. Specifically, the search delivery stage comprises the usage of the search keywords organochlorine, organophosphorus/organophosphate, pesticides/insecticides, biogenic/biosynthesized nanoparticles, photodegradation, and water pollution in various combinations with the aid of the “AND” and “OR” operators to gather several relevant

literature articles. In the first phase, a total of 845 papers were gathered. The amount of literature was reduced to 469 articles kept for additional title reading after works such as gray literature, presentations, keynotes, papers written in languages other than English, and papers with inaccessible full texts were eliminated. Only 400 papers remained eligible for additional abstract reading after that. There were only 301 articles left for the main body reading after reading the article abstract. Of these, 187 examined the photodegradation of OP and OC; these publications were retrieved in order to proceed with additional screening. Subsequently, duplicate publications and articles that did not clearly employ biogenic NPs for degradation were manually deleted throughout the main body reading process. 136 papers were ultimately chosen for an extensive examination since they met all of the inclusion criteria employed in this investigation.

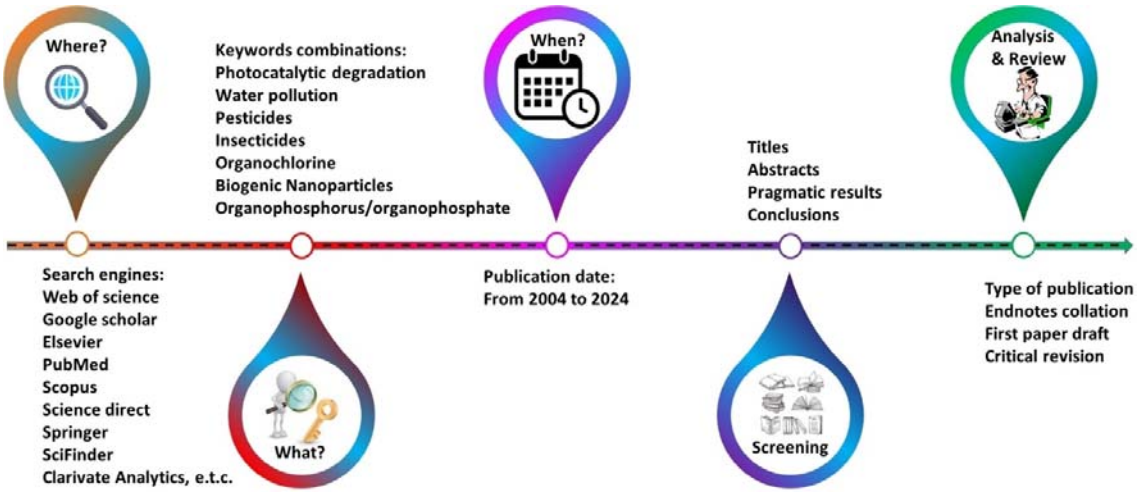

Figure 2. Methodology for selecting relevant literature. Adapted from[26] with slight modification.

3. Fate and Reaction of Organochlorine and Organophosphate in Aquatic Environment

Organophosphate pesticides are generally referred to as compounds with the organic derivatives of phosphoric acid .[40] OPs migrate through the environment in relation to the source of pollution, which progressively expands outward. This process involves three phases: water, soil, and gas, as well as physicochemical-biological processes that carry a significant ecological risk and involve volatilization, adsorption, and degradation.[41] Pollutants that have been exposed to the ground will not only immediately contaminate the soil but also surface runoff, groundwater leaching, downstream migration along the groundwater, and finally accumulation in organisms[42] (Figure 3). The more advanced organisms, the higher the amount of pesticide residues in the body and, consequently, the possible hazards to human health, according to the developmental trends in the ecological chain.[43] Pesticides including organophosphates and organochlorines alter the way fish's liver, kidney, and gill tissue normally arranges itself. Large lymphocytes and abnormal cell topologies in the nuclear erythrocytes of blood cells are additional effects of these herbicides.[44] Thousands of pesticide residues are constantly dumped into the aquatic environment in areas with extensive agricultural activity. Numerous processes, including sorption-desorption into solid particles, surface run-off, soil leaching, plant uptake, volatilization, and air deposition, control pesticide poisoning of water. The degree of these mechanisms is related to the general characteristics of the pesticides, such as their solubility and hydrophobicity, as well as environmental factors, soil/sediment type, microbial activity,

salinity, temperature, and precipitation events, and agricultural management practices, such as crop type and pesticide application rate.[45]

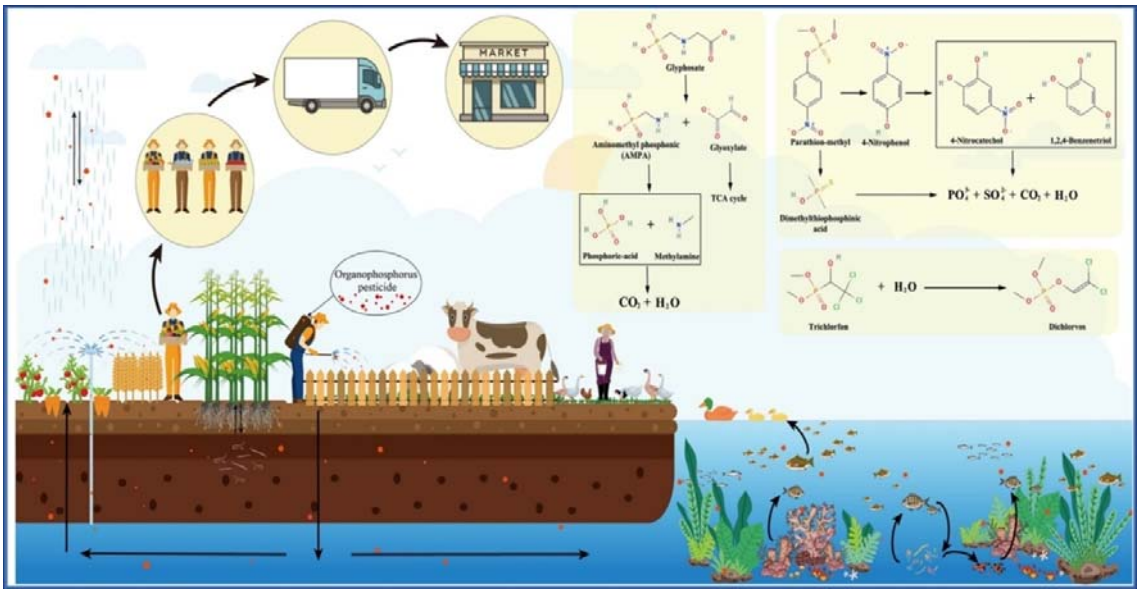

Figure 3. Fates of common organophosphates in aquatic environments.[46]

It is important to remember that when OPs enter water bodies, they become alien to the ecosystem. This means that they not only harm the environs but also openly alter the ecosystem organization and function of the water, which has a negative impact on a variety of aquatic organisms and may even lead to the extinction of some of them, reducing biodiversity and upsetting ecological balance.[47] According to published research, OPs and OCs cause oxidative stress in aquatic floras, which in turn lowers the amount of chlorophyll in the plants and prevents photosynthesis, which has an impact on plant growth. In response, the body activates specific antioxidant enzymes.[48] OPs cause cancer in addition to being mutagenic. Fish are also killed by it at greater doses of up to 0.151 ppm.[49]

4. Sources and Distribution of Organochlorine and Organophosphate in the Aquatic Body

In order to stop the growth of undesirable plants like weeds and get rid of bothersome insects and fungi, pesticides like organophosphates and organochlorines are widely employed in residential, commercial, and industrial settings as well as in agricultural production systems.[50, 51] Pesticides are mostly mobilized into bodies of water by runoff from farm land.[52] Different trophic levels and the buildup of pesticides in sediment can have harmful effects on a variety of creatures. Applying pesticides on agricultural land is one common way that organophosphate and organochlorine pesticides enter the environment. Organophosphate insecticides have a high solubility in water and enhanced adsorption in soils. As a result, contaminants build up in runoff water.[53] As runoff water enters adjacent streams and water bodies, aquatic life is continuously at risk, and farmers are exposed to these chemicals at work when they spray.[54] Organochlorine pesticides, in particular, can find their way into surface water bodies through irrigation effluents, industrial waste, runoff from farms, transportation from the application area during rainfall, agricultural wastes, and unforeseen spills.[55] Because organophosphate

pesticides, or OPs, are soluble in water, aquatic bodies are home to a large number of them. Organophosphate insecticides have been examined in drinking water, wastewater, groundwater, and surface water.[56] In addition to being essential pesticide drains, sediments have a role in the deposition of pollutants in aquatic systems.[57] OPs that have been documented in water and other aquatic systems over the years include endosulfan, dimethoate, diazinon, methyl parathion, chlorpyrifos, and malathion. OPs put aquatic habitats in extreme danger.[58] They damage aquatic microbial communities, interfere with respiration, cell development, and photosynthesis, and reduce biodiversity.[59] Organochlorine insecticides volatilize from the soil upon application, becoming suspended in the air and then returning to the soil. Additionally, they might be absorbed by plants or seep into the earth, contaminating groundwater.[60] Antioxidant enzymes and non-specific antioxidants are in charge of preserving the dynamic equilibrium between antioxidant reactions and oxidation products under normal physiological settings. When an organism's dynamic equilibrium between oxidation products and antioxidant responses is upset, oxidative stress results.[61] Numerous investigations have demonstrated the harmful consequences of organic pollutants by identifying antioxidant markers in aquatic organisms. For instance, studies have demonstrated that exposure to diazinon dramatically decreased the activities of glutathione S-transferase (GST), catalase (CAT), and total superoxide dismutase (T-SOD) in the liver of crucian carp, resulting in oxidative stress in the liver.[62] Pesticides containing organochlorines have a considerable wind-travel range before depositing on soil and water.[63] Because OCs can concentrate directly in fish tissues from their meals and surrounding water, it is challenging to quantify how the pollutant is transferred down the food chain.[64] OCs are pollutants of local, regional, and global phenomena because of their long-range transit and resistance to physical, microbiological, chemical, or photochemical destruction.[65] Research has shown that they are present in the Arctic due to long-distance travel.[66] OCs are progressively released into soil and water bodies via waste disposal, atmospheric deposition, runoff and leaching from agricultural cropland and soil, and the discharge of home and industrial sewage and runoffs.[67]

5. Photocatalytic Degradation Mechanism and Pathway

The general mechanism for the pesticide's degradation route and their degradation products are presented in Figure 4. The primary mechanism of pesticide breakdown is the interaction between active species and biogenic nanophotocatalysts, as indicated in Figure 4. As shown in Figure 5, four reactive radical species are important in pesticide photodegradation. Photogenerated holes (h^+), hydroxyl radicals (OH·), superoxide anion radicals ($O_2\cdot^-$), and electrons (e^-) are a few of the active species. The conduction band and valence band are represented by CB and VB, respectively.[68, 69] To further understand the photocatalytic mechanism and investigate active species in the process, it is imperative to determine the amount of trapped active species, as seen in Figure 4. Generally speaking, biogenic organisms (plants) reveal their active regions immediately, and h^+ and e^- can combine with O_2, adsorbed H_2O, or surface OH^- to generate $O_2\cdot$ and OH·. The extremely reactive $O_2\cdot$ and OH· radicals quickly oxidize organic molecules on the surface of NPs that have been biosynthesized.[69-71] Figure 5 shows that when biogenic NPs are exposed to sunlight or UV radiation, they absorb photons and create an e^-/h^+ pair. This pair then reacts with oxygen and water to form the $O_2\cdot$ and OH·.[70]

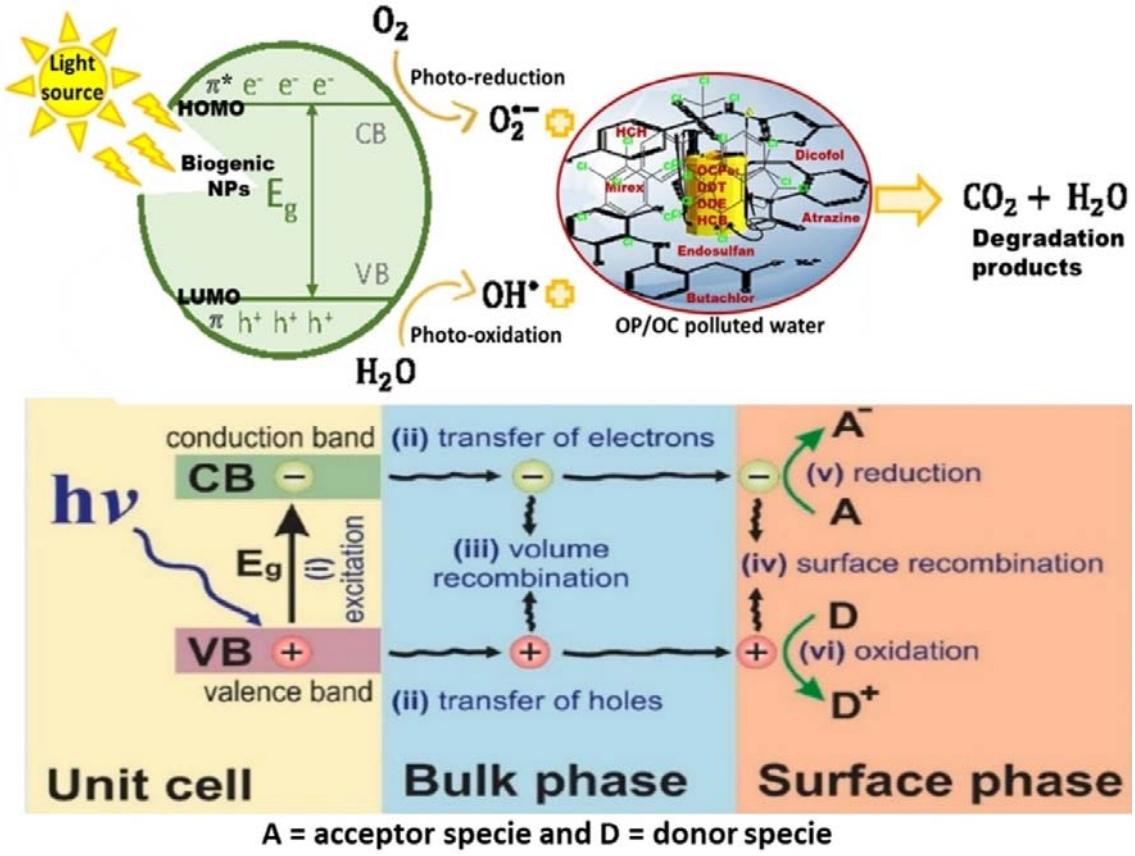

Figure 4. Overarching mechanism of biogenic nanoparticle-based photocatalytic pesticide degradation light-catalysts. (Modified from reference[13, 36]).

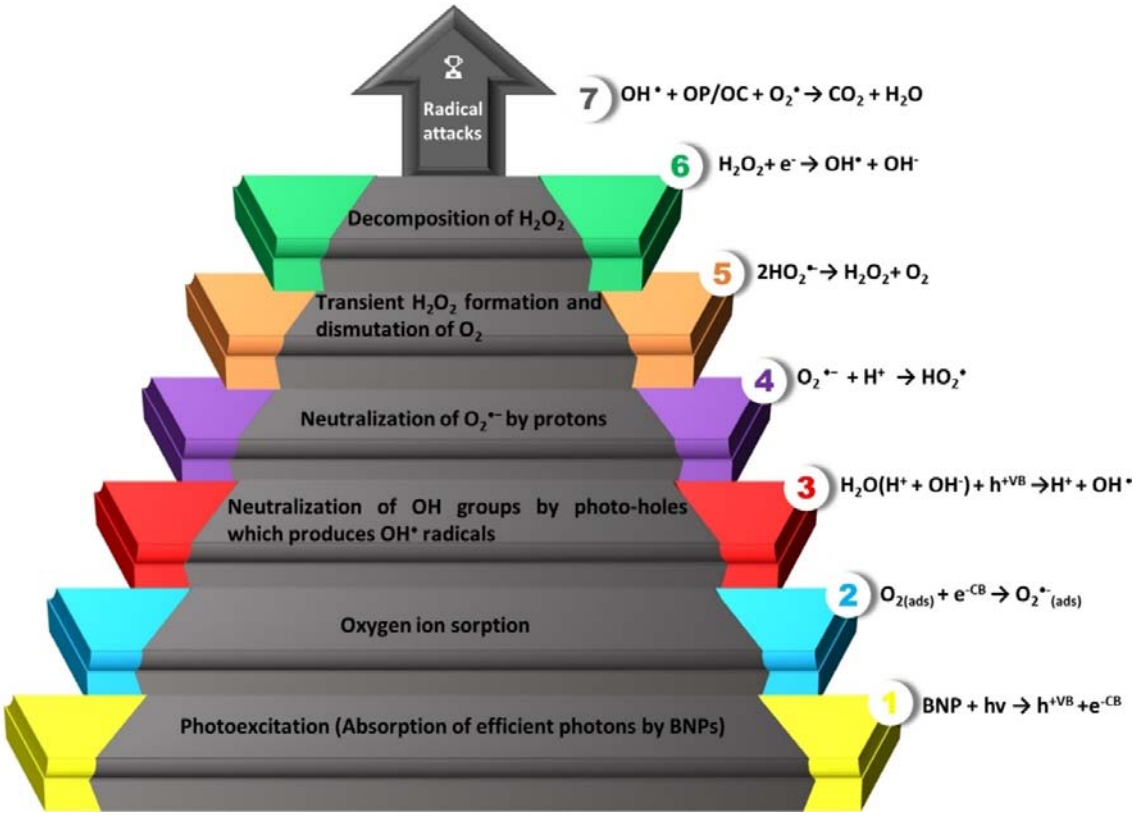

Figure 5. A possible sequential equation for photocatalytic degradation of OP/OC by biogenic NPs. Adapted from[13]

As shown in Figure 6a, h^+ played a crucial role in the breakdown of the organochlorine pesticide by converting H_2O into hydrogen ions and hydroxyl free radicals, which in turn produced 2,4-dichlorophenol (m/z=161.96) and acetic acid (m/z=61). Chlorobenzene (m/z=112.9) was produced by the created dichlorophenol interacting with H^+ ions in slurry. Some of the dichlorophenol interacted with superoxide and hydroxyl free radicals in the presence of superoxide radicals to form benzoquinone (m/z=108.02)/2-chlorobenzoquinone (m/z=141.98) and chlorobenzene-diol (m/z=144)/benzene-triol (m/z=126). In the presence of H^+ ions, some dichlorophenol underwent dechlorination, yielding phenol (m/z=94.04). Before being recognized as intermediates, all of the obtained intermediates eventually underwent ring opening and produced oxalic acid, methanolic acid, ethanoic acid, and acetaldehyde. In a similar vein, Figures 6b, 7a, and b show endosulfan and atrazine degradation pathways respectively. In the scenario of atrazine using biosynthesized $NiFe_2O_4$@ biochar, the difference in electronegativity between carbon and chlorine causes electrons to be attracted to chlorine preferentially, which causes a carbocation to form. One of the reaction's constituents, the water molecule, reacts with the carbocation to produce 4-(ethylamino)-6-(isopropylamino)-1,3,5-triazin-2-ol (m/z: 198). 6-(isopropylamino)-1,3,5-triazine-2,4-diol (m/z: 170), 6-amino-1,3,5-triazine-2,4-diol (m/z: 128), and urea (m/z: 60) are formed by further oxidation, which finally breaks down into harmless product (CO_2 and H_2O). While in the case of Endosulfan, an attack on the S=O bond is started by the peroxide active radical, which leads to the creation of an intermediate radical cation. When oxygen is present, this intermediate hydrolyzes quickly to produce an oxygen-centered radical intermediate. It then proceeds to a beta-elimination pathway via the oxygen-centered radical intermediate, generating endosulfan ether (m/z=406.

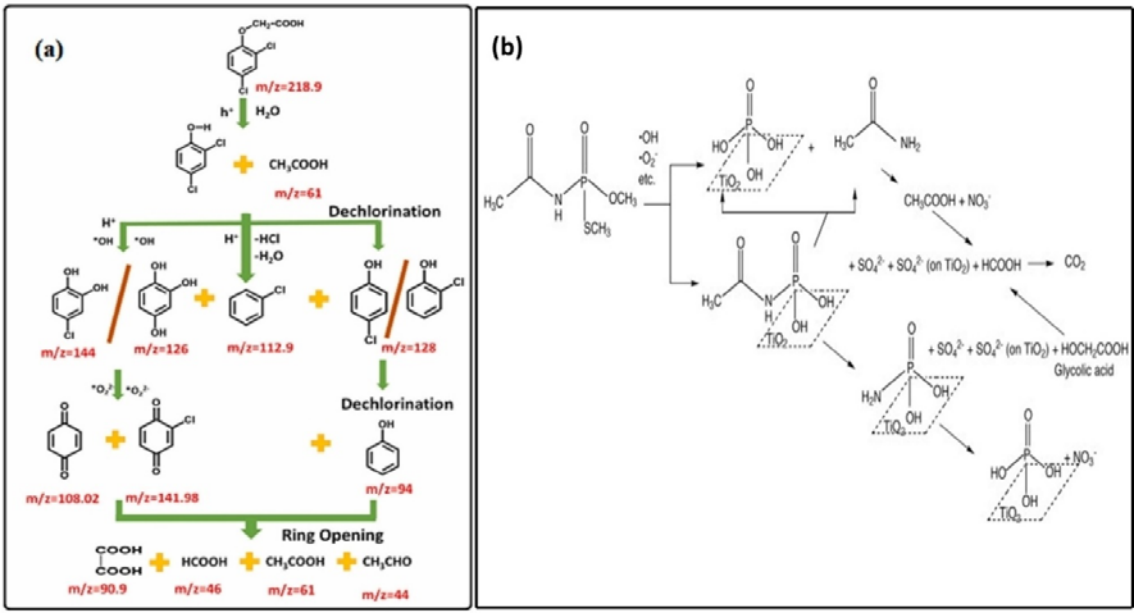

Figure 6. Tentative pathway for the photocatalytic degradation of (**a**) 2,4-D[87] **(b)** acephate compound.[88] (Adapted from references with permission from Elsevier).

Endosulfan ether undergoes an oxidative change to produce endosulfan alcohol (m/z=360), which is then transformed into endosulfan lactone (m/z=357). Through a hydrogen abstraction process, the peroxide radicals proceed to assault the by-product lactone, ultimately generating a radical with a carbon center. endosulfan lactone, endosulfan ether, endosulfan alcohol, and endosulfan sulfate as an intermediary. In addition, smaller organic molecules are produced via the oxidation and ring opening of 2,3,4,5-tetrachlorophenyl methanol (m/z=243).[72] Notably, it can be concluded that beyond the physical interaction of the BNPs and the OP/OC, chemical interaction (chemisorption) also plays a significant role in the photocatalytic degradation process. OC/OP molecules have the ability to chemisorb onto the surface of the BNPs. This involves the OC/OP molecules and the active sites on the BNP surface forming chemical interactions and the ensuing degradation processes depend heavily on the chemisorption process. Furthermore, the existence of specific functional groups on the BNP surface can facilitate various physical and chemical interactions with OP/OC including π-π stacking, H-bonding, and van der Waals forces during the adsorption stage of photocatalytic degradation operation. For example, hydroxyl and oxime groups on the surface of biogenic NPs can participate in H-bonding with OP/OC, thereby enhancing their degradation.[72, 73] In addition, some biogenic nanoparticles can form coordination complexes with OP/OC, resulting in the activation of the pesticide molecules through an electron transfer process[72] facilitating photocatalytic degradation. Also, the greater surface area increases the BNP's ability to adsorb substances, giving OP/OC molecules more active sites to interact with during the photocatalytic degradation process. In another mechanistic study, it was accentuated that because the biogenic NP supported on biochar (BC) contained oxygenated functional groups, its adsorption and photocatalytic degradation capacity was enhanced. It was opined that the OCP molecules' carbon rings might function as π-electron donors, whilst the C−O groups and C=O on the BC@BNP's surface could function as π-electron acceptors.[74] On the surface of the BC@BNPs, the O−H and −C−H aromatic groups may function as π-electron donors, whereas the OCP molecules containing Cl are electron-deficient and function as π-electron acceptors. Consequently, the BC@BNP and the OCPs may interact through the π-π electron-donor-acceptor process. This result demonstrated that the primary mechanism of adsorption that

facilitated photocatalytic degradation of OCPs by BC@BNP is the π-π electron-donor-acceptor interaction, with pore filling and hydrophobic sorption serving as secondary mechanisms.[74-76] Lastly, according to studies,[37, 81-84] the interaction between the OP/OC and photocatalyst surface is often electrostatic in nature during photocatalytic degradation[37, 73] and the photocatalytic degradation of OP/OC is affected by the BNP band gap energy, where a low band gap enhances the photocatalytic activity by encouraging efficient e^-/h^+ generation, while a high band gap may limit the photocatalytic process.[85, 86]

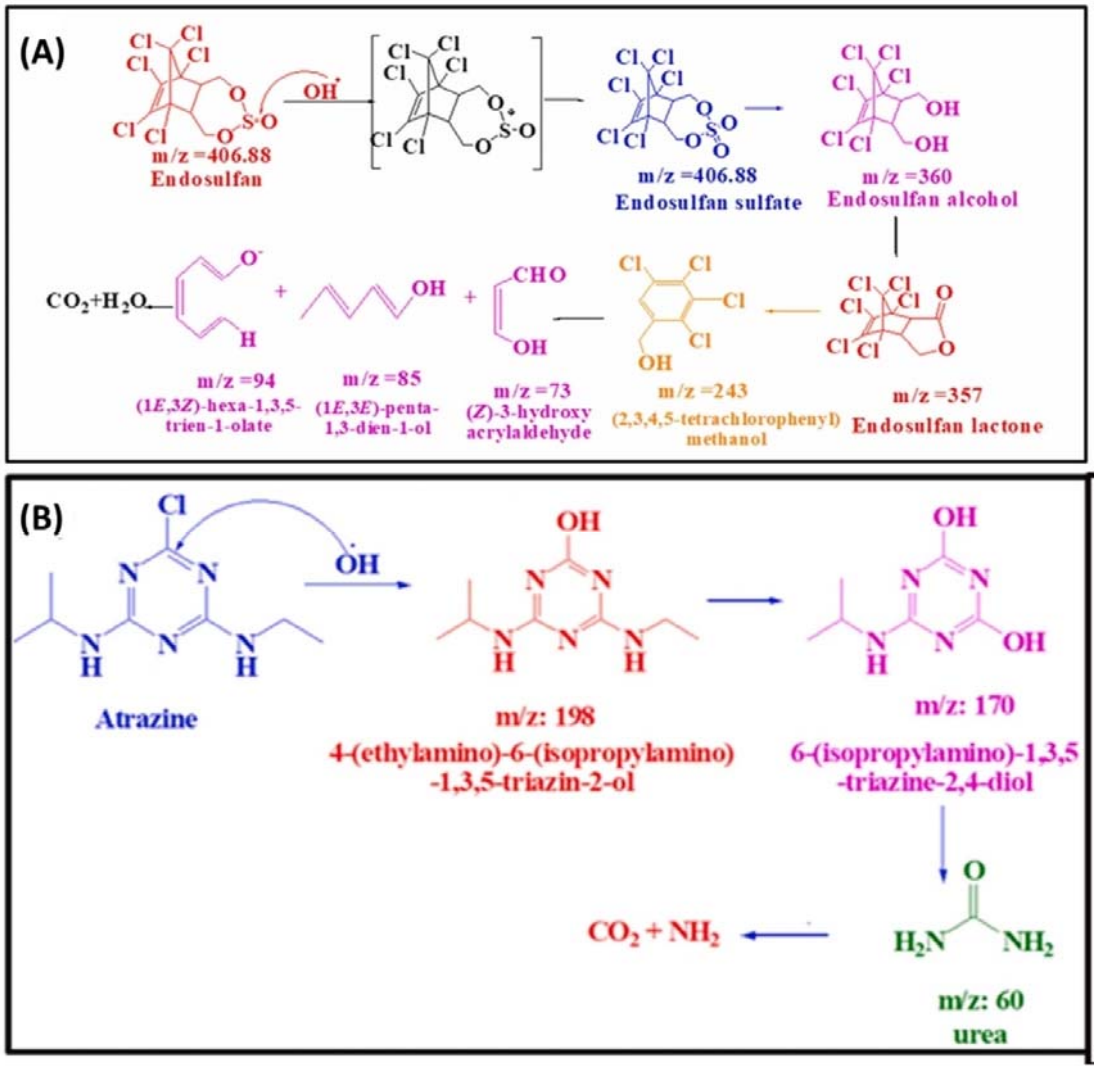

Figure 7. Possible reactions and interactions occurring during photocatalytic degradation of (a) endosulfan and (b) atrazine using biogenic $NiFe_2O_4$@biochar nanocomposite.[72]

6. Evaluation of Biogenic Nanoparticles Performance for Degradation of Organochlorine and Organophosphorus

In recent decades, as per the available literature, intensive effort has been channeled to the biofabrication of NPs and was adopted to mitigate OC/OP from contaminated water. In this

section, we discuss some of the performance of these BNPs in the context of photocatalytic degradation of OP/OC as observed in original research papers.

For example, Ningthoujam et al.[89] and colleagues conducted the biosynthesize of amorphous FeNPs with an average particle size of 25.1 nm, which were subsequently employed to investigate the degradation of lindane, an important and persistent OC pesticide, in a liquid medium. The results revealed that FeNPs at a concentration of 0.1 g/L effectively decomposed approximately 99 % of lindane within 24 hours. Moreover, the application of the FeNPs synthesized in the present study exhibited a significant reduction in the cytotoxicity associated with lindane, thereby suggesting the transformation of lindane into less harmful and simpler degradation spinoffs. Consequently, the biogenic iron NPs produced which utilize aqueous polyphenol extracts obtained from a waste product generated during food processing, hold promising potential as a remediation agent for sites contaminated with OC, such as lindane.[89] Similarly, Mehrotra et al.[90] employed a straightforward and expeditious approach for the catalytic disintegration of dichlorvos using protein-encased zero-valent iron nanoparticles with average size of 3 to 10 nm. The author devised a dependable, innocuous, environmentally conscious, and economically efficient biological technique for the formation of uniformly scattered FeNPs. The resulting spherical FeNPs exhibit substantial efficiency (>90 %) in the degradation of organophosphates.[90]

Rani et al.[91] assessed the efficacy of highly crystalline metal hexacyanoferrates (MHCFs) of Co, Ni, Zn, and Cu in breaking down specific dangerous pesticides, such as chlorpyrifos (CP), thiamethoxam (TH), and tebuconazole (TEB). Using *Sapindus mukorossi* (raw ritha), they created well-defined ZnHCF nanocubes with an average size of ~100 nm, deformed CuHCF nanocubes with an average size of <100 nm, and CoHCF and NiHCF nanospheres with an average size of <10 nm by an environmentally benign process. The chosen agrochemicals showed significant degradation when used under the following conditions: 50 mg L–1, 15 mg of MHCF photocatalyst, neutral pH, and exposure to irradiation. ZnHCF showed the highest levels of degradation (>91 %), followed by CuHCF (>85 %), NiHCF (>73 %), and CoHCF (>70 %). The large BET surface area and zeta potential of ZnHCF are responsible for this tendency. The catalysts' acidic surfaces exhibited a remarkably high degradation of CP (>83 %), TH (>76 %), and TEB (>70 %), most likely due to the unbound electrons present in their structures. The interaction of H_2O or O_2 with the e^- and h^+ pairs produced on the catalyst surface when exposed to sunlight led to the creation of remarkably potent ·OH, the primary agent responsible for oxidation. This agent is capable of decomposing and eventually mineralizing intricate compounds. Upon treatment with MHCF photocatalysts, the target compounds underwent complete breakdown and produced minor, non-harmful spinoffs, namely (Z) but-2-enal, 3-aminopropanoic acid, and pyridin-3-ol, which further demonstrated the photocatalytic potential of MHCFs.[91]

In another investigation, Pushkar and Sevak[92] discovered that biogenic (synthesized using Neem leaf extract) spherical Fe-oxide nanoparticles with average particle size ranging from 21.03 to 80 nm exhibited significant efficacy in eliminating DDT from the surrounding environment. After two hours of incubation, equilibrium was obtained and the highest level of DDT degradation was reached at pH 3. The initial DDT adsorbate concentration had a significant impact on how well it was removed as well. The as-biosynthesized Fe_3O_4 nanoparticles effectively removed a significant amount (>88 %) of DDT, with a peak concentration of 500 ppm of DDT. Consequently, the investigation ultimately posited that Fe-oxide nanoparticles have the potential to be employed for the efficient eradication of DDT from the surrounding environment.[92] This is similar to the results of Rani et al.,[93] using iron oxide

NPs fabricated using green tea extract and supported on biochar (BC) made from waste peels of *Citrus limetta*. The biogenic spherical BC@Fe_2O_3 nanohybrid with mesoporous network, average size of 8 nm, and enhanced porosity with a surface area of 74 m^2/g was employed to photocatalytically degrade endosulfan and ethion pesticides. The experiments were carried out under specific conditions, with a pollutant concentration of 50 mg/L, a catalytic dose of 25 mg, and an acidic environment, while utilizing natural sunlight. The biogenic BC@Fe_2O_3 nanohybrid demonstrated remarkable efficiency in the breakdown of pesticides (94 % for endosulfan and 91 % for ethion) compared to bare spherical biogenic F_2O_3 counterpart with a surface area of 38 m^2/g that gave 50 % and 45 % for both endosulfan and ethion respectively. The BC@Fe_2O_3 effectiveness was attributed to several factors, including a higher zeta potential(−22.5 mV), enhanced surface area, BC support, porosity, and lower band gap value of 1.8 eV, which can be attributed to its interactive characteristics and semiconducting behavior.[93]

In another study, Batool et al.[74] employed a distinctive biogenic spherical nanocomposite, Fe^0-B_{RtP}, consisting of zero-valent iron (Fe^0) supported on biochar. This biogenic NP was fabricated from *Nephelium lappaceum* fruit peel waste and has an average size of 20 to 80 nm, surface area of 109.57 m^2/g, total pore volume of 0.24 m^2/g and pore diameter of 8.84 nm. Six OCs were eliminated simultaneously from an aqueous medium using it: endosulfan (96 %), hexachlorobenzene (>96 %), heptachlor (>96 %), aldrin (99 %), o,p'-DDT (99 %), and p,p'-DDT (99 %). Notably, Furthermore, a Fe0-BChe nanocomposite that was chemically produced was made ready for comparison. The capacity of Fe0-BRtP and Fe0-BChe nanocomposites to adsorb and dechlorinate OCs in an aqueous solution was shown by batch studies. As shown in Figure 9, at an initial pH of 4, they were able to obtain degradation rates of up to 96–99 % and 83–91 % within 120 and 150 minutes, respectively. However, as shown in Figure 8, the reactivity of the Fe^0-B_{Che} nanocomposite decreased by a factor of two after exposure to air for one month, whereas biogenic Fe^0-B_{RtP} remained nearly unchanged.[74] It can be deduced that the outer layer of polyphenols from the green *N. lappaceum* peel extract is what kept the biogenic Fe^0-B_{RtP} nanoparticles supported on biochar relatively stable in the air. The biogenic Fe^0-B_{RtP} nanoparticles were completely enclosed by the polyphenols, which also prevented oxidation and led to inactivation. However, throughout the aging process, chemically fabricated Fe^0-B_{Che} nanoparticles oxidize in the air.[74, 94, 95]

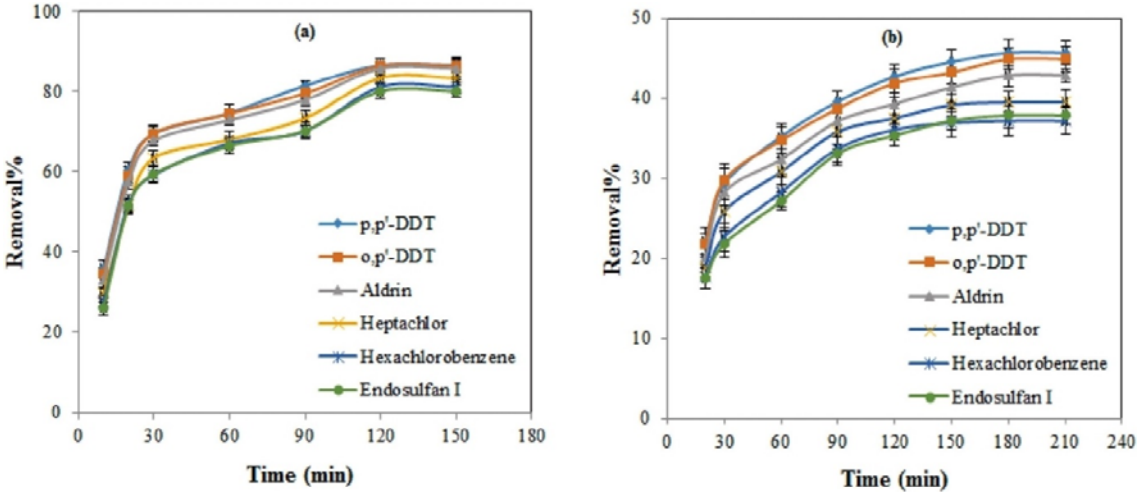

Figure 8. Efficacy of one month-aged biogenic (a) and non-biogenic (b) zero-valent iron supported on BC for the removal of OCPs.[74]

In another study, El-Said[96] utilized two distinct types of extract derived from the leaves of green tea, namely total extraction and tannin extract, as reductants to develop a rapid, straightforward, and single-step synthesis approach for creating mesoporous and quasi-spherical hybrid silica nanoparticle/iron oxide nanocomposites through the deposition of iron oxide onto mesoporous silica nanoparticles. The findings of this study demonstrated that the aforementioned mesoporous silica nanoparticle/iron oxide nanocomposite with surface area of 93 m^2/g and pore volume of 0.31 cm^3/g showed a notable removal capacity for lindane pesticides, resulting in a removal efficiency of up to 98 %. It was further observed that the adsorption process was contingent upon the pH level, with the greatest removal efficiency achieved at a pH of 7. Moreover, the degradation capacity of the nanocomposite increased with increasing temperature, implying that the degradation process was endothermic. Consequently, the developed nanocomposite displayed promise as a nanophotocatalyst for eliminating organochlorine pesticides from aqueous solutions owing to its substantial adsorption capacity and ease of recovery using an external magnetic field.[96] A close observation was recorded by Paknikar et al.[97] in the degradation of lindane. Rod-like FeS nanoparticles with an average particle size of ~200 nm were fabricated using a wet chemical process, followed by stabilization with a biopolymer that was obtained from the basidiomycetous fungus *Itajahia sp*. In just eight hours, the biogenic nanoparticles showed an amazing capacity to break down lindane (5 mg/l) with a 94 % efficiency. The BNPs completely degrade the lindane pesticide in one hour under a later microbiological treatment. The latter procedure made it easier for biogenic FeS to aggregate and be easily removed by filtration. The difficulty of removing chlorinated contaminants from water sources presents a tremendous opportunity for which our novel integrated nano-biotechnological technique has great promise as an effective, safe, and economical solution.[97] Chawla's research group[87] combined *Curcuma longa* extract and $BiVO_4$ to fabricate a very efficient heterostructure flower-shaped biogenic photocatalyst with an average particle size of 79 nm, surface of 35.140 m^2/g and pore size of 3.082 nm. The resultant catalyst showed that OCs could be efficiently broken down in a water-based media. In particular, when compared to pristine BiVO4 (2,4-D:45.94 % and 2,4-DP:28.18 %) under visible-light irradiation for 120 minutes, the photocatalytic degradation of 2,4-D (2,4-dichlorophenoxy acetic acid) increased from 45.94 % to 90.23 %, and the degradation of 2,4-DP (2-(2,4-dichlorophenoxy propionic acid) increased from 35.56 % to 70.52 % after the addition of C. longa on bismuth vanadate. In addition, these outcomes show higher efficiency when compared to previously manufactured nanomaterials. The creation of numerous interfaces between BiVO4 and *C. longa* is responsible for the considerable boost in pollutant degradation by impeding the recombination of photogenerated charge carriers. After conducting investigations on radical quenching and analyzing intermediates, it was concluded that the degradation of OCs entailed the presence of +ve hole, hydroxyl radical, and superoxide radical. The fragmentation process was pH-dependent, and when the pH didn't fluctuate, the degradation was at its best.[87] Similarly, Choudhary et al.[98] employed a deformed spherically shaped biogenic nanocomposite material consisting of nitrogen-doped Bi_2O_3@SnO_2 to eliminate the pesticides ethion (ET) and toxaphene (TP). The biogenic N-Bi_2O_3@SnO_2 nanocomposite with an average particle size of 10–80 nm was biosynthesized using leaves of *A. indica*, and demonstrated superior degradation capabilities, achieving removal efficiencies of 96 % for ET and 90 % for TP with catalytic dosage of 30 mg, at an initial pesticide concentration of 2 mg/L, and under sunlight irradiation at a neutral pH level compare to distorted spherical and cubical biogenic Bi_2O_3 and SnO_2 that demonstrated a low photocatalytic degradation efficiency as shown in Figure 10 under the same experimental conditions. The biogenic N-Bi_2O_3@SnO_2 nanocomposite exhibits improved photocatalytic efficiency because of its greater surface area (75 $m^2\ g^{-1}$), the synergetic effect of Bi_2O_3 and SnO_2 with a surface area of 30 $m^2\ g^{-1}$ and 45 $m^2\ g^{-1}$ respectively, higher negative zeta potential value (−23.4 mV),

and lower bandgap energy (2.1 eV).[98] Table 2 presents the photocatalytic degradation of OP and OC pollutants using green biogenic NPs, as reported in the literature. Conclusively, it can be observed from the above discussion and as shown in Figures 9 and 10 that the photocatalytic degradation performance is governed by pragmatic parameters like pH, temperature, BNPs dose, initial OC/OP concentration, and irradiation time and after the optimum peak, the performance begins to drop sharply or remain unchanged.

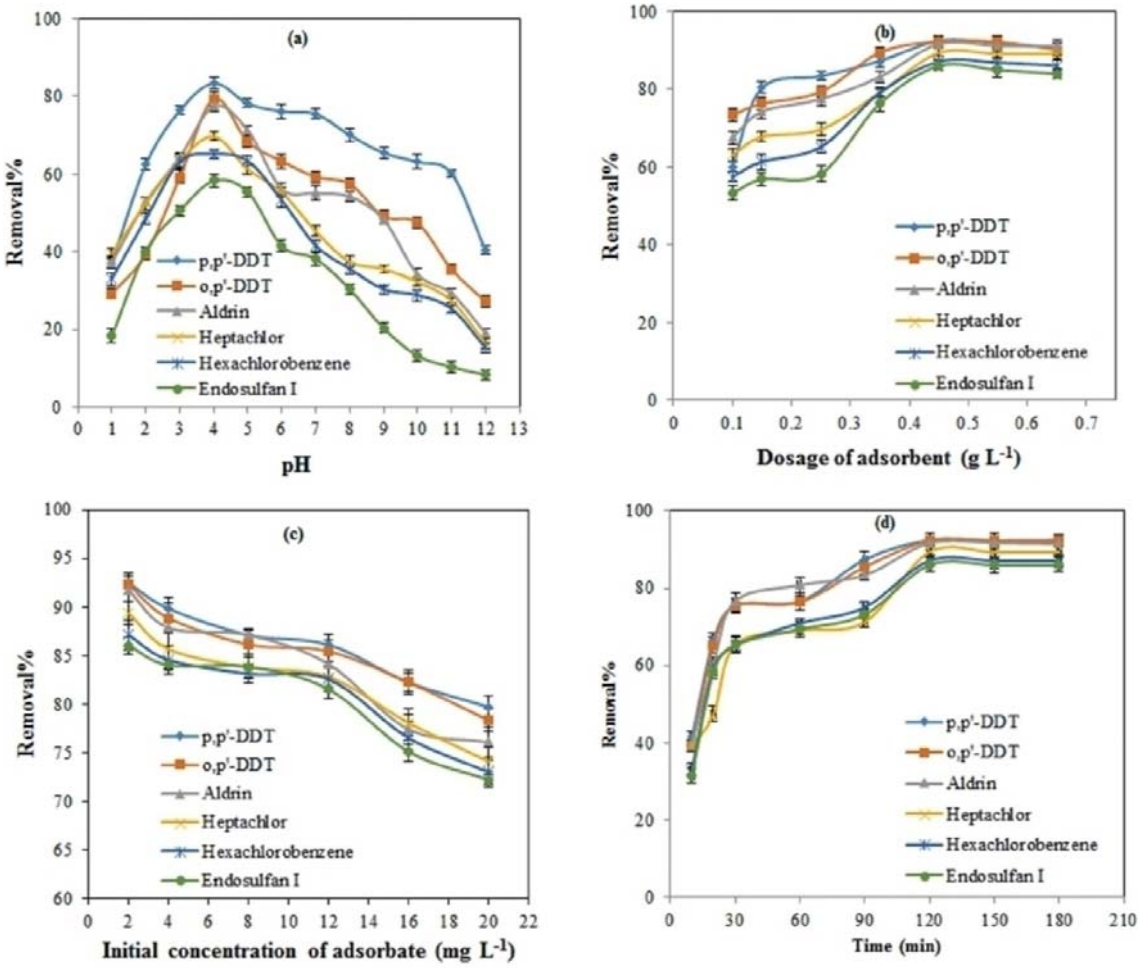

Figure 9. Effect of (a) pH, (b) biogenic Fe^0-B_{RtP} dose, (c) initial OC concentration, and (d) residence time on OCPs photodegradation by biogenic Fe^0-B_{RtP} nanocomposites.[74]

Table 2. Summary of degradation efficiency of some biosynthesized nanoparticles for organochlorine and organophosphorous pollutants.

BNPs	Biogenic source	Shape and size(nm)	OC and OP	DE (%)	DT (mins)	References
TiO_2@$CdMgFe_2O_4$	Guar gum	Spherical 18–34	Endosulfan	95	210	[100]
BC@$NiFe_2O_4$	*Murraya koenegii* leaves	Spherical <100	Atrazine	98	30	[72]
TiO_2	*Coffea arabica* L.	–	Paraquat	66.3	90	[101]
TiO_2@$CdMgFe_2O_4$	Guar gum	Spherical 18–34	DDE	89	210	[100]
CuO	*Capparis decidua* leaf	Flower	Lambda-cyhalothrin	99	180	[99]
SnO_2	*A. indica* leaf extract	Distorted cubical 10–80	Ethion	55	360	[98]
SnO_2	*A. indica* leaf extract	Distorted cubical 10–80	Toxaphene	50	360	[98]
Ag/Cu	*Carica papaya*	star-like 150	Chlorpyrifos	>60	168*	[102]
NiO	*Capparis decidua* leaf	Flower	Lambda-cyhalothrin	89	180	[99]
BC@$NiFe_2O_4$	*Murraya koenegii* leaves	Spherical <100	Endosulfan	92	30	[72]
Fe_3O_4	Neem leaves extract	Spherical 21.03–80	DDT	90.2	120	[92]
$BiVO_4$	*Curcuma longa*	Flower 79	2,4-D	90.2	120	[87]

Zn@HCF	*Sapindus mukorossi*	Cubes ~100	Chlorpyrifos	98	12*	[91]
Cu@HCF	*Sapindus mukorossi*	Distorted cubes <100	Chlorpyrifos	91	12*	[91]
Ni@HCF	*Sapindus mukorossi*	Spherical <10	Chlorpyrifos	85	12*	[91]
Co@HCF	*Sapindus mukorossi*	Spherical <10	Chlorpyrifos	83	12*	[91]
Fe	pomegranate fruit peels	Amorphous 25.1	Lindane	~99	24*	[89]
Fe	Yeast extract	Spherical 3–10	Dichlorvos	>90	60	[90]
Ag	Chitosan	25–50	Imidacloprid	85	–	[103]
Au	*Rhizopus oryzae*	Crystalline 10	Malathion	~85	24*	[104]
Au	*Rhizopus oryzae*	Crystalline 10	Chlorpyrifos	~99	24*	[104]
Au	*Rhizopus oryzae*	Crystalline 10	Dimethoate	>75	24*	[104]
Au	*Rhizopus oryzae*	Crystalline 10	Parathion	>85	24*	[104]
Cu−ZnO	*Melia azedarach* leaf extract	Irregular 4–8	Chlorpyrifos	91	240	[105]
Fe_3O_4	*euphorbia cochinchinensis* extract	Spherical	Doxorubicin hydrochloride	80.2	48*	[106]

		10–30				
$BiVO_4$	*Curcuma longa*	Flower 79	2,4-DP	70.52	120	[87]
SiO_2@ Fe_3O_4	green tea leaf	quasi-spherical	Lindane	>99	420	[96]
FeS	Basidiomycetous fungus, Itajahia sp	Rod ~200	Lindane	~100	540	[97]
Nitorgen-Bi_2O_3@SnO_2	*A. indica* leaf extract	Deformed spherical 10–80	Ethion	96	360	[98]
Nitorgen-Bi_2O_3@SnO_2	*A. indica* leaf extract	Deformed spherical 10–80	Toxaphene	90	360	[98]
Fe	*Dalium guineense* stem bark extract	Spherical	α-BHC	~95.5	180	[107]
Fe	*Dalium guineense* stem bark extract	Spherical	β-BHC	~40	180	[107]
Fe	*Dalium guineense* stem bark extract	Spherical	γ-BHC	~36	180	[107]
Fe	*Dalium guineense* stem bark extract	Spherical	Heptachlor	~17	180	[107]
Fe	*Dalium guineense* stem bark extract	Spherical	δ-BHC	~68	180	[107]
Fe	*Dalium guineense* stem bark extract	Spherical	Aldrin	~48	180	[107]
Fe	*Dalium guineense* stem bark extract	Spherical	Heptachlor epoxide	~100	180	[107]
Fe	*Dalium guineense* stem bark extract	Spherical	γ-Chlordane	~81.3	180	[107]
Fe	*Dalium guineense* stem bark extract	Spherical	α-Chlordane	~100	180	[107]
Fe	*Dalium guineense* stem bark extract	Spherical	Endosulfan I	~84.4	180	[107]
Fe	*Dalium guineense* stem bark extract	Spherical	P,p'-DDE	~85.4	180	[107]
Fe	*Dalium guineense* stem bark extract	Spherical	Dieldrin	~77.3	180	[107]
Fe	*Dalium guineense* stem bark extract	Spherical	Endrin	~100	180	[107]
Fe	*Dalium guineense* stem bark extract	Spherical	P,P'-DDD	~82	180	[107]
Fe	*Dalium guineense* stem bark extract	Spherical	Endosulfan II	~100	180	[107]
Fe	*Dalium guineense* stem bark extract	Spherical	P,P'-DDT	~100	180	[107]
Fe	*Dalium guineense* stem bark extract	Spherical	Endrin aldehyde	~100	180	[107]
Fe	*Dalium guineense* stem bark extract	Spherical	Endosulfan sulphate	~100	180	[107]
Fe	*Dalium guineense* stem bark extract	Spherical	Methoxychlor	~100	180	[107]
Fe	*Dalium guineense* stem bark extract	Spherical	Endrin ketone	~100	180	[107]
Fe@CMC	*Dalium guineense* stem bark extract	Spherical	α-BHC	~100	180	[107]

		11.95				
Fe@CMC	*Dalium guineense* stem bark extract	Spherical 11.95	β-BHC	~95	180	[107]
Fe@CMC	*Dalium guineense* stem bark extract	Spherical 11.95	γ-BHC	~91.1	180	[107]
Fe@CMC	*Dalium guineense* stem bark extract	Spherical 11.95	Heptachlor	~70.1	180	[107]
Fe@CMC	*Dalium guineense* stem bark extract	Spherical 11.95	δ-BHC	~25	180	[107]
Fe@CMC	*Dalium guineense* stem bark extract	Spherical 11.95	Aldrin	~86.4	180	[107]
Fe@CMC	*Dalium guineense* stem bark extract	Spherical 11.95	Heptachlor epoxide	~100	180	[107]
Fe@CMC	*Dalium guineense* stem bark extract	Spherical 11.95	γ-Chlordane	~21	180	[107]
Fe@CMC	*Dalium guineense* stem bark extract	Spherical 11.95	Endosulfan I	~100	180	[107]
Fe@CMC	*Dalium guineense* stem bark extract	Spherical 11.95	Dieldrin	~60.2	180	[107]
Fe@CMC	*Dalium guineense* stem bark extract	Spherical 11.95	Endrin	~28	180	[107]
Fe@CMC	*Dalium guineense* stem bark extract	Spherical 11.95	P,P'-DDD	~83	180	[107]
Fe@CMC	*Dalium guineense* stem bark extract	Spherical	Endosulfan II	~100	180	[107]

		11.95				
Fe@CMC	*Dalium guineense* stem bark extract	Spherical 11.95	P,P'-DDT	~87	180	[107]
Fe@CMC	*Dalium guineense* stem bark extract	Spherical 11.95	Endrin aldehyde	~93.33	180	[107]
Fe@CMC	*Dalium guineense* stem bark extract	Spherical 11.95	Endosulfan sulphate	~19	180	[107]
Fe@CMC	*Dalium guineense* stem bark extract	Spherical 11.95	Methoxychlor	~100	180	[107]
Fe@CMC	*Dalium guineense* stem bark extract	Spherical 11.95	Endrin ketone	~100	180	[107]
ZnO	*Cissus quadrangularis* leaf extract	Hexagonal 15–20	Dieldrin	93.12	120	[108]
ZnO@ maize cobs AC	*Cissus quadrangularis* leaf extract	Foam	Dieldrin	99.76	120	[108]
Ag	*P. hibiscicola*	–	Chlorpyrifos	88.49	–	[109]
Ag	*P. hibiscicola*	–	Malathion	75.79	–	[109]
Ag	*P. hibiscicola*	–	Dichlorvos	78.2	–	[109]
Ag	*P. hibiscicola*	–	Profenofos	64.1	–	[109]
$CuFe_2O_4$	Arabic Gum-grafted-polyamidoxime	37	Chlorpyrifos	>90	15	[73]
rGO@Ag	*Curcubita maxima* leaf extract	Spherical	Chlorpyrifos	76	105	[110]
Fe@BC	*Nephelium lappaceum* fruit peel	Spherical 20–80	Endosulfan	96	120	[74]
Fe@BC	*Nephelium lappaceum* fruit peel	Spherical 20–80	Hexachlorobenzene	>96	120	[74]
Fe@BC	*Nephelium lappaceum* fruit peel	Spherical 20–80	Heptachlor	>96	120	[74]

Fe@BC	*Nephelium lappaceum* fruit peel	Spherical 20–80	Aldrin	~99	120	[74]
Fe@BC	*Nephelium lappaceum* fruit peel	Spherical 20–80	o,p'-DDT	~99	120	[74]
Fe@BC	*Nephelium lappaceum* fruit peel	Spherical 20–80	p,p'-DDT	~99	120	[74]
citrus limetta BC@ Fe_2O_3	green tea extract	spherical 8	Endosulfan	94	300	[93]
Fe_2O_3	green tea extract	spherical 8	Endosulfan	50	300	[93]
Fe_2O_3	green tea extract	spherical 8	Ethion	45	300	[93]

*=carboxymethyl cellulose=CMC, AC=activated carbon, BC=biochar, HCF=hexacyanoferrate, reduced graphene oxide=rGO, BNPs=Biosynthesized nanoparticles, DE=Degradation efficiency, DT=Degradation time, OP=Organochlorine, OP=Organophosphorus/Organophophate, α-BHC=alpha Benzene hexachloride, β-BHC=beta Benzene hexachloride, γ-BHC=gamma Benzene hexachloride, δ-BHC=delta Benzene hexachloride, gamma=γ, alpha=α, P,p'-DDE=dichloro-diphenyl chloroethane, P,P'-DDD=dichlorodiphenyldichloroethane, P,P'-DDT=dichlorodiphenyltrichloroethane, 2,4-D=2,4-dichlorophenoxy acetic acid, 2,4-DP=2-(2,4-dichlorophenoxy)-propionic acid.

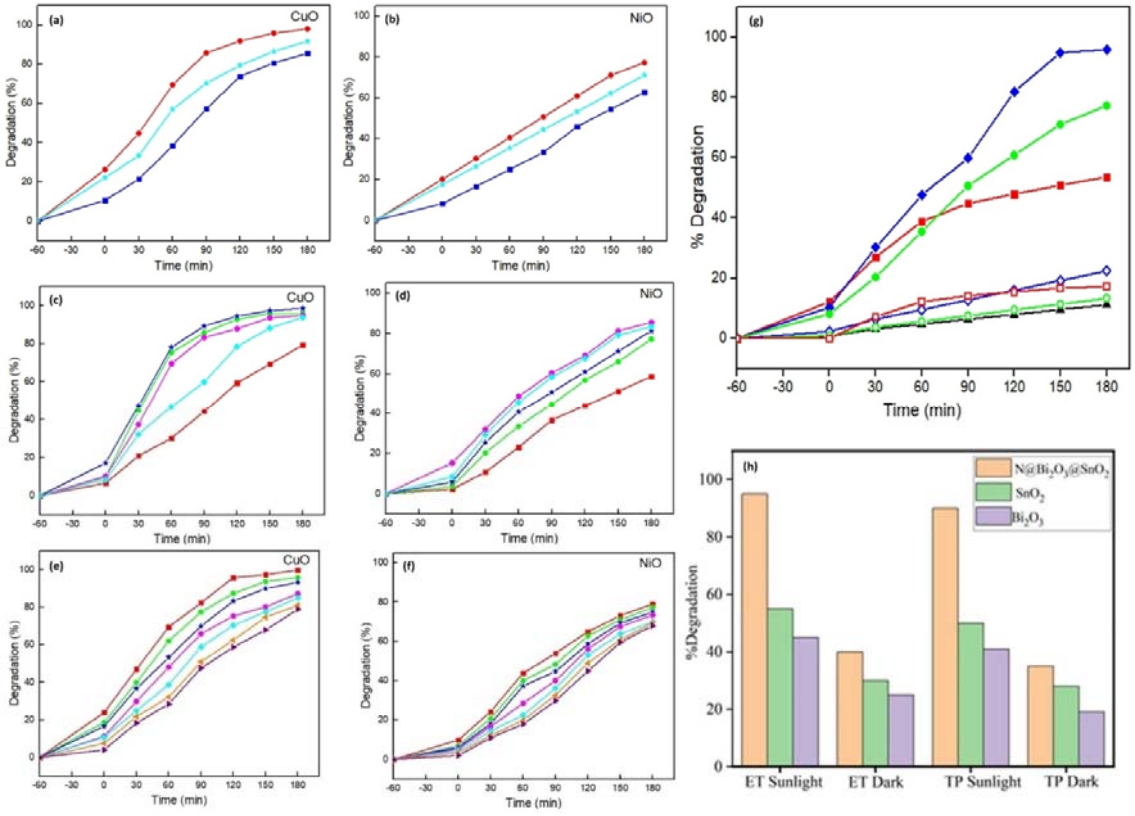

Figure 10. impact of pH on Lambda-cyhalothrin photocatalytic degradation using biogenic (**a**) CuO, (**b**) NiO NPs, at initial pH: (▪) pH=5, (•) pH=7, and (★) pH=9, Impact of BNPs dosage ((▪) 1 mg L^{-1}, (•) 2 mg L^{-1}, (★) 3 mg L^{-1}, (⬢) 4 mg L^{-1}, and (⧫) 5 mg L^{-1}) on Lambda-cyhalothrin photocatalytic degradation using biogenic (**c**) CuO, (**d**) NiO NPs, Impact of initial concentration of Lambda-cyhalothrin ((▪) 10 mg L^{-1}, (•) 20 mg L^{-1}, (★) 30 mg L^{-1}, (⬢) 40 mg L^{-1}, (⧫) 50 mg L^{-1}, (‣) 60 mg L^{-1}, and (▲) 70 mg L^{-1} on Lambda-cyhalothrin photocatalytic degradation using biogenic (**e**) CuO, (**f**) NiO NPs, (g) Degradation of Lambda-cyhalothrin at optimum conditions using biogenic (⧫,◊) CuO, (•,○) NiO, and TiO_2 (▪,□) under UV-light irradiation (filled symbols) or in the dark (empty symbols) and (▲) direct photolysis,[99] (h) Degradation efficiency of Toxaphene and Ethion under sunlight irradiation and without sunlight irradiation (in the dark) using biogenic Nitorgen-Bi_2O_3@SnO_2, Bi_2O_3 and SnO_2 NPs.[98]

7. Equilibrium Isotherm and Kinetic Model of OP and OC Photocatalytic Degradation

In explaining the interaction between the pollutant and the nanophotocatalyst, the adsorption isotherm is a crucial modeling approach. It explains the existing connection between a substance's quantity per unit mass adsorbed by the nanophotocatalyst at a fixed temperature and its equilibrium solution concentration.[111] It is of utmost importance to carry out the design and optimization of the adsorption process in a bid to develop an acceptable isotherm model for the adsorption process. A variety of models have been developed by various researchers for the removal (adsorption) of toxins. Some of these include Freundlich,[112] Langmuir,[110, 113] and Dubinin-Kaganer-Radushkevich (DKR)[114, 115] amongst several others. From Table 3, it can be seen that the Langmuir model appears to be the most common best-fit isotherm when studying adsorptions using BNPs. This is largely attributed to the practicability and ease of term linearization associated with it, wherein different nanophotocatalyst materials show homogeneity that is maintained even on agitation of the solution.[105] The Langmuir isotherm presumes that solute molecules will continuously form a monolayer on the nanophotocatalyst's surface.[116, 117] Additionally, the tiny size of the BNPs greatly increases the possibility of just

Table 3. An overview of fittest kinetic and isothermal model of various OP and OC degraded by biogenic NPs.

BNPs	Biogenic source	OC and OP	Best-fit-Isotherm	R^2	Best-fit Kinetics	R^2	References
BC@$NiFe_2O_4$	*Murraya koenegii* leaves	Endosulfan	Langmuir	0.99	PFO	0.98	[72]
BC@$NiFe_2O_4$	*Murraya koenegii* leaves	Atrazine	Langmuir	0.99	PFO	0.98	[72]
Fe_3O_4	*Euphorbia cochinchinensis* extract	Doxorubicin hydrochloride	Freundlich	0.994	PSO	0.9486	[112]
Cu−ZnO	*Melia azedarach* leaf extract	Chlorpyrifos	–	–	PFO	0.99	[105]
Zn@HCF	*Sapindus mukorossi*	Chlorpyrifos	Langmuir	0.981	–	–	[91]
Cu@HCF	*Sapindus mukorossi*	Chlorpyrifos	Langmuir	0.962	–	–	[91]
Ni@HCF	*Sapindus mukorossi*	Chlorpyrifos	Langmuir	0.971	–	–	[91]
Co@HCF	*Sapindus mukorossi*	Chlorpyrifos	Langmuir	0.966	–	–	[91]
ZnO@ maize cobs AC	*Cissus quadrangularis* leaf extract	Dieldrin	Langmuir	0.8929	PSO	0.9988	[108]
$CuFe_2O_4$	Arabic Gum-grafted-polyamidoxime	Chlorpyrifos	Langmuir	0.949	PSO	0.99	[73]
rGO@Ag	*Curcubita maxima* leaf extract	Chlorpyrifos	Langmuir	0.994	–	–	[110]
Fe@BC	*Nephelium lappaceum* fruit peel	Endosulfan	Langmuir	0.9948	PSO PFO	0.9701 0.9687	[74]
Fe@BC	*Nephelium lappaceum* fruit peel	Hexachlorobenzene	Langmuir	0.9977	PSO PFO	0.9855 0.9758	[74]
Fe@BC	*Nephelium lappaceum* fruit peel	Heptachlor	Langmuir	0.9983	PSO PFO	0.9833 0.9665	[74]
Fe@BC	*Nephelium lappaceum* fruit peel	Aldrin	Langmuir	0.9977	PSO PFO	0.9948 0.9881	[74]
Fe@BC	*Nephelium lappaceum* fruit peel	o,p'-DDT	Langmuir	0.9963	PSO PFO	0.9929 0.9829	[74]
Fe@BC	*Nephelium lappaceum* fruit peel	p,p'-DDT	Langmuir	0.9972	PSO PFO	0.9938 0.9966	[74]
$CdMgFe_2O_4$@TiO_2	Guar gum	Endosulfan	Langmuir	0.98	PFO	0.98	[100]
$CdMgFe_2O_4$@TiO_2	Guar gum	DDE	Langmuir	0.98	PFO	0.98	[100]
citrus limetta BC@ Fe_2O_3	green tea extract	Endosulfan	Langmuir	0.98	PFO	–	[93]
citrus limetta BC@ Fe_2O_3	green tea extract	Ethion	Langmuir	0.99	PFO	–	[93]
Fe_2O_3	green tea extract	Endosulfan	Langmuir	0.98	PFO	–	[93]
Fe_2O_3	green tea extract	Ethion	Langmuir	0.99	PFO	–	[93]

PFO=Pseudo-first order, PSO=Pseudo-second order, R^2=Correlation coefficient, carboxymethyl cellulose=CMC, AC=activated carbon, HCF=hexacyanoferrate, reduced graphene oxide=rGO, BNPs=Biosynthesized nanoparticles, DE=Degradation efficiency, OP=Organochlorine, OP=Organophosphorus/Organophosphate, α-BHC=alpha Benzene hexachloride, β-BHC=beta Benzene hexachloride, γ-BHC=gamma Benzene hexachloride, δ-BHC=delta Benzene hexachloride, gamma=γ, alpha=α, P,p'-DDE=dichloro-diphenyl chloroethane, P,P'-DDD=dichlorodiphenyldichloroethane, P,P'-DDT=dichlorodiphenyltrichloroethane, 2,4-D=2,4-dichlorophenoxy acetic acid, 2,4-DP=2-(2,4-dichlorophenoxy)-propionic acid.

monolayer uptake. The active sites on the BNPs are energetically homogenous, thus favouring the process. In assessing the energetics of the adsorption operation as per the order and rate constant, kinetic adsorption data is employed. BNPs have been applied to the removal of organochlorine and organophosphate pollutants. Pseudo-first-order (PFO)[100, 105] and pseudo-second-order (PSO)[73, 112, 118] models can be used to simulate the elimination kinetics of these contaminants. The results in Table 3 show that the degradation of OC and OPs by biogenic nanoparticles is in tandem with the PSO kinetics model. The premise of this idea is that the rate-limiting phase in valence forces may be chemical adsorption, which is the sharing or exchange of electrons (a chemical link) between the nanophotocatalyst and adsorbate.[119] The fact that the PSO fits best illustrates how the amount of OC and OPs that are finally adsorbed depends on the interaction between their concentration in the aqueous phase and the accessibility of their active sites on the surface of the nanophotocatalyst The increasing surface area of the biogenic nanophotocatalyst enhances the chemical adsorption, ensuring that the process is chemically irreversible.[120, 121] The R^2 value gave an insight into the best-fit model, where a value of 1 indicates a perfect fit.

8. Recyclability and Regenerability

The success of nanonanophotocatalysts from ecological, industrial, financial, and practical perspectives is heavily influenced by the factors of regenerability and recyclability.[122-125] Additionally, this mechanism serves as a beneficial tool in the development of a dependable, environmentally friendly, and economically viable photocatalytic mineralization of pollutants such as OC and OP in the environment.[115, 120, 121] In particular, the cost factor plays a significant role in the production of new nanosorbents. Consequently, the regeneration of used nanosorbents holds great significance in the process of the removal of pollutants from aqueous solutions.[126] Regeneration refers to the degradation-desorption process utilized to recover a depleted nanonanophotocatalyst from a reaction mixture. This process involves the removal of the adsorbed substance, such as OC and OP, from the nanonanophotocatalyst surface by applying a suitable eluting solvent. Regeneration of wasted nanonanophotocatalysts offers notable advantages. Moreover, it advances our knowledge of the fundamental processes driving the degradation and photocatalytic degradation process.[117, 127] In recent studies,[128, 129] a variety of approaches have been employed for the rejuvenation of depleted nanonanophotocatalysts. Among these methods, the chemical method has been found to be preferable over thermal and biological methods due to its advantageous attributes which include but are not limited to being uncompounded, economical, and swift regeneration within a short time. The subsequent paragraphs will delve into the latest research on the recovery of the photocatalysts from BNPs-loaded nanonanophotocatalysts, encompassing the utilization of different eluting agents and the subsequent regeneration of the nanonanophotocatalysts. These findings are summarized in Table 4, which also includes the individual BNPs' degradation capacity for OC and OP throughout multiple degradation-desorption cycles. The regeneration process of Fe^0-BSNP from the OC-loaded biogenic nanophotocatalysts by Batool et al.[130] involved the utilization of 10 mL of n-hexane as the desorbing agent. The process of regenerating depleted functionalized Fe^0-BNPs was carried out by adjusting the pH of the solution using either 0.1 M hydrochloric acid or sodium hydroxide solution. A quantity of 0.01 g of nanophotocatalyst was employed, and a contact period of 1 hour was implemented to effectively desorb all OC pesticides simultaneously. The reusability of the Fe^0-BSNP was assessed through the performance of many degradation-desorption cycles. At a pH of 4 and a concentration of 2 mg L^{-1} for each OC-pesticide solution, the cyclic degradation process was investigated for a contact time of 120 mins. Based on the obtained results, it was witnessed that the degradation capacity of the Fe^0-BSNP nanoparticles did not exhibit a significant reduction following five consecutive

Table 4. Summary of regenerability and recyclability studies.

BNPs	Biogenic source	OC and OP	Eluent	DE @ n=1	Cycle no	DE @ nth cycle	References
BC@$NiFe_2O_4$	*Murraya koenegii* leaves	Atrazine	Acetone and deionized H_2O	98	8	88	72
CuO	*Capparis decidua* leaf	Lambda-cyhalothrin	Distilled H_2O and EtOH	99	5	>70	99
NiO	*Capparis decidua* leaf	Lambda-cyhalothrin	Distilled H_2O and EtOH	89	5	>60	99
BC@$NiFe_2O_4$	*Murraya koenegii* leaves	Endosulfan	Acetone and deionized H_2O	92	8	86	72
Nitorgen-Bi_2O_3@SnO_2	*A. indica* leaf extract	Ethion	Distilled H_2O and acetone	95	8	81	98
Nitorgen-Bi_2O_3@SnO_2	*A. indica* leaf extract	Toxaphene	Distilled H_2O and acetone	90	8	78	98
$CuFe_2O_4$	Arabic Gum-grafted-polyamidoxime	Chlorpyrifos	Ethanol	89.7	3	85.01	73
Fe@BC	*Nephelium lappaceum* fruit peel	Endosulfan	Distilled H_2O and n-hexane	94	5	>85	74
Fe@BC	*Nephelium lappaceum* fruit peel	Hexachlorobenzene	Distilled H_2O and n-hexane	95	5	>85	74
Fe@BC	*Nephelium lappaceum* fruit peel	Heptachlor	Distilled H_2O and n-hexane	97	5	>90	74
Fe@BC	*Nephelium lappaceum* fruit peel	Aldrin	Distilled H_2O and n-hexane	**97**	**5**	>90	74
Fe@BC	*Nephelium lappaceum* fruit peel	o,p'-DDT	Distilled H_2O and n-hexane	**98**	**5**	>90	74
Fe@BC	*Nephelium lappaceum* fruit peel	p,p'-DDT	Distilled H_2O and n-hexane	**98**	**5**	>90	74
$CdMgFe_2O_4$@TiO_2	Guar gum	Endosulfan	Distilled water and acetone	**94**	**8**	87	100
$CdMgFe_2O_4$@TiO_2	Guar gum	DDE	Distilled water and acetone	**88**	**8**	80	100
citrus limetta BC@ Fe_2O_3	green tea extract	Endosulfan	Centrifugation, water and acetone	**94**	**7**	87	93
citrus limetta BC@ Fe_2O_3	green tea extract	Ethion	Centrifugation, water and acetone	**91**	**7**	86	93

carboxymethyl cellulose=CMC, AC=activated carbon, HCF=hexacyanoferrate, reduced graphene oxide=rGO, BNPs=Biosynthesized nanoparticles, DE=Degradation efficiency, OP=Organochlorine, OP=Organophosphorus/Organophophate, α-BHC=alpha Benzene hexachloride, β-BHC=beta Benzene hexachloride, γ-BHC=gamma Benzene hexachloride, δ-BHC=delta Benzene hexachloride, gamma=γ, alpha=α, P,p'-DDE=dichloro-diphenyl chloroethane, P,P'-DDD=dichlorodiphenyldichloroethane, P,P'-DDT=dichlorodiphenyltrichloroethane, 2,4-D=2,4-dichlorophenoxy acetic acid, 2,4-DP=2-(2,4-dichlorophenoxy)-propionic acid.

degradation-desorption cycles. The Fe-BNPs underwent a process of regeneration on five separate occasions and were thereafter subjected to testing in order to assess their potential for reuse across a span of five cycles. However, it was observed that there was no substantial decrease in the degradation efficiency of OC-pesticides for the regenerated Fe^0-BNPs. The observed phenomenon may be attributed to the inhibition of iron oxide layer development, which occurs as a consequence of the encapsulation of Fe^0-BNPs by polyphenol from the plant material. Therefore, it is evident that the green synthesized Fe^0-NPs exhibit characteristics of being an environmentally sustainable and cost-effective nanophotocatalyst.[130] The investigation carried out by Choudhary et al.[98] focused on examining the efficacy of a hybrid nanocomposite Bi_2O_3@SnO_2 in mitigating Ethion and Toxaphene pesticide concentrations under solar irradiation. The pesticide samples were subjected to centrifugation, followed by washing with distilled water and acetone. Subsequently, the samples were dried using a hot air oven in order to assess the potential for reusing the catalysts. The degradation efficiency of Bi_2O_3@SnO_2 declined from 95 % to 81 %, while the efficiency of Toxaphene decreased from 90 % to 78 % when compared to Bi_2O_3 (75–63 %) and SnO_2 (56–46 %). This decrease in efficiency confirms the effective reusability of Bi_2O_3@SnO_2. The researchers found that the hybrid nanocatalyst exhibited reusability for a minimum of eight cycles in the same reaction scenario while retaining its catalytic activity and sustained generation of active species. The utilization of hybrid nanocomposites was supported by the PXRD spectrum, hence justifying their unhindered application for up to the 8th cycle.[98]

In the study conducted by Rani et al.,[131] the team examined the reusability of the photocatalysts Fe_2O_3 and BC@Fe_2O_3, under optimum conditions, for the removal of endosulfan and ethion pesticides through solar irradiation. In order to regenerate the catalysts from the pesticide samples, the solution underwent centrifugation, followed by the recovery of the solid portion using filtration. The solid was next subjected to repeated cleaning cycles using distilled water and acetone. The catalyst underwent a drying process in a hot air oven for a duration of 8 hours at a temperature of 60 °C, after which it was subsequently reused. The findings of the study demonstrated the high efficacy of the catalyst in the elimination of Endosulfan, with removal rates ranging from 94 % to 87 %. Similarly, the catalyst exhibited significant effectiveness in removing Ethion, with removal rates ranging from 91 % to 86 % for the BC@Fe_2O_3 nanoparticle. Furthermore, it has been demonstrated that hybrid photocatalysts (BC@Fe_2O_3) produced by environmentally friendly methods exhibit exceptional reusability and stability, suggesting their potential for long-term sustainability. The potential suitability of the modified BC@ Fe2O3 nanohybrid as a catalyst for industrial applications is supported by its reusability (n=7), ability to facilitate charge separation, stability, and high surface activity.[131] In another experiment, $CuFe_2O_4$ magnetic nanoparticles were regenerated using ethanol as a desorbing agent by Hassanzadeh-Afruzi et al..[126] By submerging and swirling the BNP in ethanol at ambient temperature for a duration of 4 hours, the chlorpyrifos was been desorbed from the biosorbent. Consequently, the chlorpyrifos compound was introduced into the solution, followed by the separation of the nanophotocatalyst using a magnet. The nanophotocatalyst was subsequently subjected to multiple washes using distilled water and then dried in preparation for subsequent degradation-desorption tests. Following three cycles of use, the degradation and desorption percentages of the $CuFe_2O_4$ magnetic nanoparticles decreased from 89.7 and 86.99 to 85.01 and 81.05, respectively. This indicates that the biosorbent is a good fit and works well as a nano- photocatalyst for the removal of chlorpyrifos from contaminated aqueous solutions. The findings from the degradation-desorption trials indicated that the synthetic nanophotocatalyst consistently retained its high efficacy in chlorpyrifos removal, with just a marginal decrease of around 4 % observed after the three consecutive cycles. In addition, the inclusion of $CuFe_2O_4$ magnetic nanoparticles (MNPs) inside the hydrogel matrix

has resulted in the development of a magnetic hydrogel that can be repeatedly utilized. This characteristic enables the hydrogel to be easily removed from aqueous solutions during all degradation processes.[126] Keshu et al.[100] have reported the excellent and promising reusability (n=9) of $CdMgFe_2O_4@TiO_2$ nanocomposite in the effective removal of endosulfan and DDE pesticides from contaminated solution under natural sunlight conditions. The regeneration of the expended nanonanophotocatalyst was done using the same solvent as previously utilized by Choudhary et al..[98] Following each experimental trial, the photocatalyst was subjected to centrifugation in order to separate it from the sample. Subsequently, the catalyst was subjected to multiple washes using distilled water and acetone as eluting agents. Finally, the catalyst was placed in a hot air oven at a temperature of 60 °C for a duration of 6 hours to assess its potential for reuse. During the investigation of reusability, it was observed that the efficiency of the photocatalyst reduced from 94 and 88 % to 87 and 80 % for ES and DDE respectively when using the guar gum incorporated $CdMgFe_2O_4@TiO_2$ polymeric nanocomposite. This little decrease in efficiency confirms the effective reusability of the photocatalyst. The nanocatalyst demonstrated consistent effectiveness over nine consecutive uses, employing identical removal settings, while maintaining its photocatalytic degradation efficiency and sustained production of active species. The observed little decrease in the percentage of pesticide degradation observed in each successive cycle is similar to what was observed in Figure 11[98-100] and can perhaps be related to the cleansing of the nanomaterials due to the development of resistance among nanoparticles.[100] Pesticides have the potential to accumulate on the surface of conglomerate nanoparticles after undergoing nine cycles, resulting in the inhibition of photon absorption at active sites. This inhibition subsequently leads to a decrease in degradation efficiency. However, careful observation of the PXRD spectrum of the guar gum incorporated $CdMgFe_2O_4@TiO_2$ after the 3rd, 5th, and 9th cycle, provides evidence supporting the absence of any perceived structural changes in the polymeric nanocomposites. To corroborate this assertion, the pesticide solution that has undergone photodegradation is analyzed for the presence of Cd^{2+} ions using atomic absorption spectroscopy. The result revealed the absence of Cd^{2+}, thus confirming the stability of the photocatalyst.[100] There are several reasons for the observed marginal decline in the regenerated nanonanophotocatalyst's effectiveness in subsequent degrading studies. This phenomenon could be attributed to the intense contact between the OC and OP and the nanonanophotocatalyst. Furthermore, during the elution or regeneration process, the surface architectural functional groups of the nanonanophotocatalyst may sustain minor damage. Moreover, a reduction in the quantity of open and accessible active sites on the nanonanophotocatalyst surface may result from a tiny loss of mass during the regeneration process as well as the eluent of OC and OP molecules occupying certain degrading sites. These findings have been supported by previous studies.[65, 127, 131, 132]

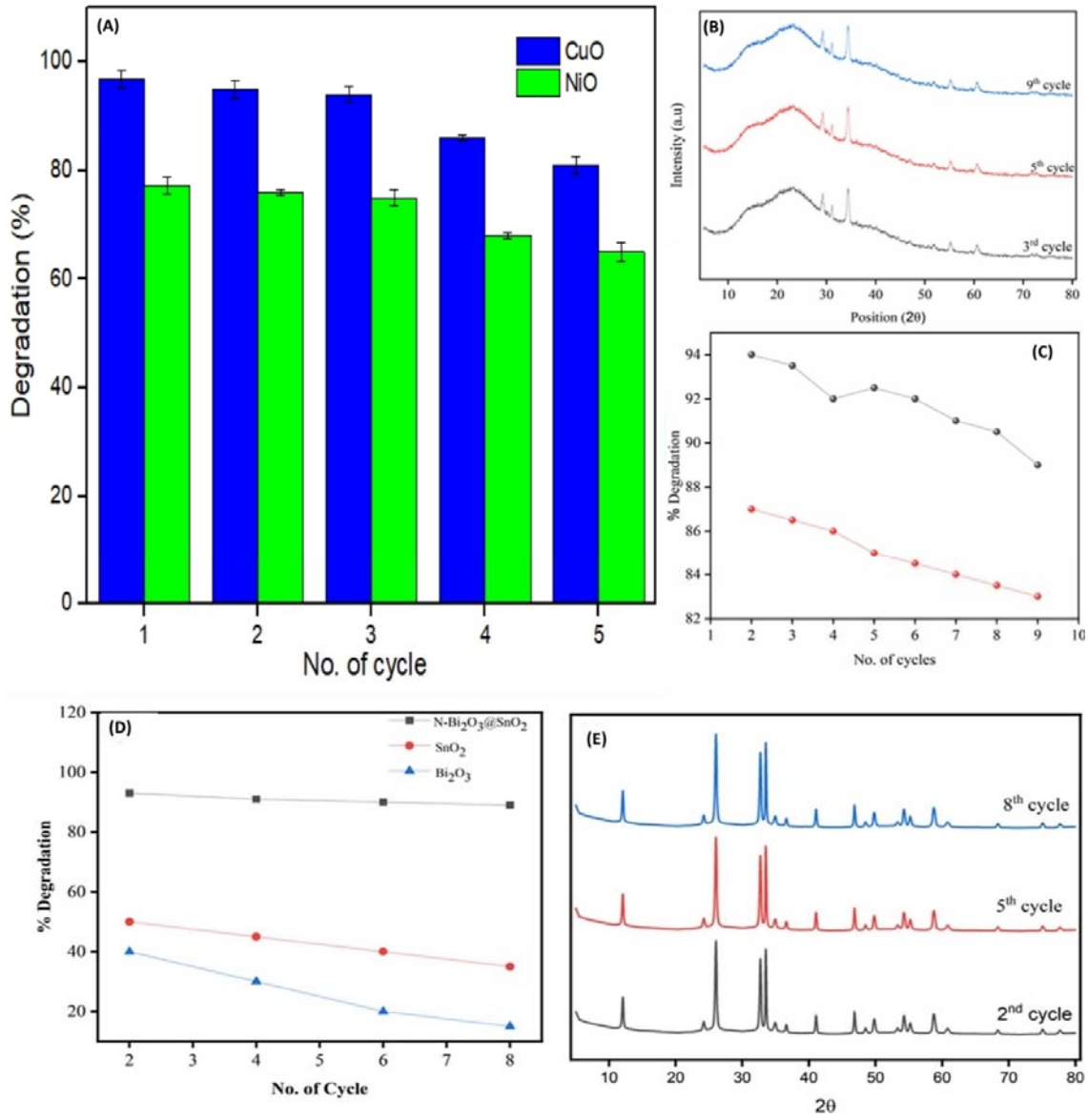

Figure 11. (a) Recyclability test of biogenic NiO and CuO NPs against Lambda-cyhalothrin,[99] (b) PXRD data of reused biogenic GG-$CdMgFe_2O_4$@TiO_2 nanocomposite,[100] (c) Recyclability test of biogenic GG-$CdMgFe_2O_4$@TiO_2 nanocomposite,[100] (d) Recyclability test of biogenic nanocomposite,[98] (e) PXRD data of reused biogenic nanocomposite.[98]

According to the regenerability and recyclability data collected in Table 4, a biogenic nanonanophotocatalyst can be recycled and repurposed for OC and OP degradation an average of roughly six cycles, with the lowest number of recyclability being three and the highest number being eight. After the nth cycle, a nanonanophotocatalyst's average degradation capacity is higher than 78 %. Several eluents have been studied to help desorb OP and OC from used nanophotocatalysts Among these are ethanol,[126] distilled water and acetone,[93, 98] distilled water and n-hexane,[130] and centrifugation, water and acetone.[131] However, the most frequently used eluent is distilled water and n-hexane. Table 4 presents a comprehensive overview of desorption and reuse as documented in the available literature.

9. Problematic Issues and Future Research Direction

Notably, from this review, a number of research works have produced noteworthy outcomes when it comes to the use of biosynthesized NPs for the photocatalytic degradation of OC and OP pesticides, nevertheless, there are still some problematic issues to overcome in the field of environmental stewardship. These challenges provide an array of interesting hotspots for future research. The first major problematic issue for researchers when using biogenic NPs for photocatalysis degradation is increasing the biogenic NPs' spectrum sensitivity to visible light. Most biogenic NPs synthesized today are only active in the UV and areas close to the UV, where their effectiveness is restricted due to an energy mismatch with the visible band of the solar spectrum. Thus, future work should be directed towards biosynthesizing superior biogenic NPs that are incredibly active and efficient in the visible spectrum in direct sunlight. Secondly, future researchers should focus more on the regenerability and reusability of biogenic NPs to improve their real-life applicability and adoption, as there is a shortage of studies in this area, at least in the context of this review subject. Furthermore, immobilizing biogenic NPs on an inert surface (such as ceramics, quartz, or glass) can improve their recyclability. Future researchers can also look at the circular economy possibilities of expended biogenic NPs; maybe they can be recycled as materials for supercapacitors after being reused several times in photocatalytic degradation operations. Another significant problematic issue with biogenic NPs is that some of their negative effects, such as increased cytotoxicity, oxidative stress, and cell proliferation inhibition, have not been well studied and controlled, particularly after absorbing harmful contaminants like OC and OP during photocatalytic degradation operations. If the biogenic NPs can't be properly eluted and reused, the loss of expended NP is unavoidable and can lead to deadly socio-ecological and economic issues owing to the fact that the leaked biosynthesized NPs will lead to weighty resource spendthrift, financial setbacks, and sizable ecotoxicity through biomagnification and bioaccumulation of the leaked expended biogenic NPs within the bio-network. Moreover, huge amounts of phytochemicals can leak into aquatic systems from the biogenic NPs, and this might be dangerous to aquatic life if it is too much for them to handle. Also, the exact chemical structure of various phytocompounds participating in the synthesis of biogenic NPs needs to be probed in order to have a better understanding of their mechanistic role in the photocatalytic degradation process. Even though certain biomolecules, like proteins and glycolipids, have been demonstrated to control the size and shape of biogenic NPs, an improved comprehension of the biochemical pathways and biomolecules involved is still a pending research task. Thus, managing the properties of biogenic NPs is still a key challenge.[133, 134] In the future, efforts should be focused on the application of artificial intelligence to forecast the capping and reduction abilities of biogenic entities, as this will help to reduce ambiguity and guesswork when attempting to identify which plant will be a superior reducing agent for the biosynthesis of a given NP.[13] Furthermore, in order to properly apply biogenic NPs to real-world problems such as environmental governance, a more thorough understanding of their durability, stability, and photocatalytic degradation productivity over a longer period, such as a month or a year, is required. A further intriguing practical challenge to the widespread use of biogenic NPs and photocatalytic degradation is scaling up, and this should be looked into by upcoming investigators. Future research endeavors can look at integrating transformative front-line techniques like artificial intelligence, including machine learning, and molecular simulations. These forward-thinking techniques may allow future researchers to fully investigate the intricacies of biogenic NPs and their role in the photocatalytic degradation of OC and OP contaminants, as they provide insights that are often not possible with traditional bulk experiments or spectroscopic studies. Future studies should take advantage of exploring the synergistic impact of mixing two or more biogenic entities (plant-microorganism,

microorganism-microorganism, plant-fungi, plant-plant, plant-algae, etc.)[12] as this may result in faster and more effective bio-reduction of metals during the NPs biosynthesis operation. Furthermore, there is not much work on the use of genetically engineered biogenic entities for the synthesis of biogenic NPs. Investigating genetically engineered biogenic entities is worthwhile as it can improve the ability to assemble and absorb metals during the production of green NPs. Additionally, as observed from this review, only the commonly used kinetics and isotherm models like PSO, PFO, Langmuir, and Freundlich were applied; thus, we suggest the exploration of other models like Redlich-Peterson, Ritchie, Hills, Scatchard, Crank, Toth, and Jovanovich, Flory-Huggins, Frusawa and Smith, Bangham, pseudo-nth-order, internal diffusion model, etc. in the future. This will enhance the knowledge of the adsorption process that occurs during photocatalytic degradation operations and, hence, the knowledge of photodegradation in a way. Lastly, future research on the use of biogenic NPs for photocatalytic degradation is advised to include financial analysis because investors and industrial engineers are very interested in this important topic.

10. Conclusions

Organochlorine and organophosphorus pesticides are deadly contaminants that disturb the peace of environmental sustainability, aquatic systems, and human health. Herein, we holistically presented the photocatalytic degradation of OP and OC contaminants in an aquatic environment using biosynthesized NPs, and the degradation efficiency was empirically analyzed and appraised in conjunction with the regenerability and reusability potential of different regenerants and eluents. Several main findings were derived. Firstly, it was found that biosynthesized NPs are promising green recyclable photocatalysts for degrading aquatic pollutants like OP and OC, as it was observed that even at the nth regenerability cycle, most of the biogenic NPs still maintain over 80 % degradation efficiency. Secondly, it was found that the maximum degradation proficiency is 100 %, while the least degrading time required is 1 hour, and this is a clear testament to the remarkable potential of biogenic NPs in the domain of environmental remediation. It was also revealed that most of the photocatalytic degradation data fit the Langmuir isotherm model better, which indicates that the adsorption process involved during photocatalytic degradation is monolayer at the surface of the biogenic NPs, while the kinetic follows both PFO and PSO, with PFO coming to the fore in most studies, which shows that the main mechanism of adsorption that occurs during the photocatalytic degradation of OC and OP using biogenic NPs is physical adsorption. Furthermore, it was discovered that plant extract is the most widely employed capping agent or bioreductant for the biosynthesis of various biogenic NPs reported, and this might be due to the availability and ease of access of plants as a biogenic entity and the plethora of phytochemicals containing hydroxyl, carbonyl, and other oxygenated functional groups present in the plant.[135, 136] This study also discloses that Au, Ag, and Fe-based biogenic NPs are the most widely studied biogenic NPs for OC and OP degradation, and this was perceived to be a result of their intrinsic excellent properties like fast light response, good surface area, and so on. It was also found that the dominant radicals participating in the degradation of OP and OC using biogenic NPs are ·OH and O_2· and this radical dominance was enhanced by the hydroxyl and oxygenated functional groups present in the biogenic entities employed for the biosynthesis of the biogenic NPs. Though there has been a lot of progress in our knowledge of the photocatalytic degradation of OP and OC utilizing biogenic NPs, there are still many areas that need to be researched and improved upon. To ensure the practical application of these biogenic NPs, important variables, including cost, biosafety, and compatibility with industrial environments, need to be meticulously investigated. To close these knowledge gaps and generate cost-effective and environmentally friendly green nanomaterials for the full mineralization of OP

and OC, more research is required. Conclusively, this work offers a threefold significant advantage in terms of environmental protection, sustainable agricultural practices, and water security, and the findings gained from this study may also be useful to readers, engineers, and industries that are interested in adopting photocatalytic degradation for achieving robust and viable wastewater treatment strategies towards the actualization of sustainable development goals number 6 and 14.

CRediT Author Statement

Stephen Sunday Emmanuel.: Conceptualization, Methodology, Writing- Original draft preparation, Supervision, Validation, Project administration, Writing- Reviewing and Editing, **Ademidun Adeola Adesibikan**.: Writing- Original draft preparation, Validation, Writing- Reviewing and Editing, **Christopher Olusola Olawoyin**.: Writing- Original draft preparation, Validation, Writing- Reviewing and Editing, **Mustapha Omenesa Idris.**: Writing- Original draft preparation, Validation, Writing- Reviewing and Editing **Abdulbasit A Aliyu**.: Writing- Original draft preparation, Validation **Abdulrahman Itopa Suleiman**.: Writing- Original draft preparation, Validation

Conflict of interests

There are no declared conflicts of interest, either financial or non-financial.

Data Availability Statement

Data sharing is not applicable to this article as no new data were created or analyzed in this study.

References

1. P. Mondal, *Int. J. Bioresour. Sci.* 2018, 5, 81–89.
2. N. E. Fedorova, M. V. Egorova, A. S. Rodionov, *Public Heal. Life Environ.* 2021, 29, 48–54.
3. M. A. Islam, S. M. N. Amin, M. A. Rahman, A. S. Juraimi, M. K. Uddin, C. L. Brown, A. Arshad, *Environ. Nanotechnology, Monit. Manag.* 2022, 18, 100740.
4. W. Wang, X. Wang, N. Cheng, Y. Luo, Y. Lin, W. Xu, D. Du, *TrAC Trends Anal. Chem.* 2020, 132, 116041.
5. M. Arienzo, A. Masuccio, L. Ferrara, *Arch. Environ. Contam. Toxicol.* 2013, 65, 396–406.
6. W. H. Organization, Public Health Impact of Pesticides Used in Agriculture, World Health Organization, 1990, 128.
7. N. Dhankhar, J. Kumar, *Mater. Today: Proc.* 2023, 766, 1–5.
8. P. Rajak, S. Roy, A. Ganguly, M. Mandi, A. Dutta, K. Das, S. Nanda, S. Ghanty, G. Biswas, *J. Hazard. Mater. Adv.* 2023, 10, 100264.
9. K. Bano, S. Kaushal, P. P. Singh, *Polyhedron* 2021, 209, 115465.
10. H. Huang, C. Xia, D. Liang, Y. Xie, F. Kong, J. Fu, Z. Dou, Q. Yang, W. Suo, Q. Zhang, Z. Meng, *Chem. Eng. J.* 2022, 431, 134113.
11. M. Omenesa, H. Kim, A. Ali, M. Nasir, M. Ibrahim, *Sustain. Energy Technol. Assessments* 2022, 52, 102183.
12. S. S. Emmanuel, A. A. Adesibikan, O. D. Saliu, *Appl. Organomet. Chem.* 2023, 37, e6946.

13. S. S. Emmanuel, A. A. Adesibikan, O. D. Saliu, E. A. Opatola, *Plant Nano Biol.* 2023, 100024.
14. S. S. Emmanuel, C. O. Olawoyin, I. D. Ayodele, O. J. Oluwole, *J. Organomet. Chem.* 2023, 122767.
15. S. S. Emmanuel, A. A. Adesibikan, E. A. Opatola, C. O. Olawoyin, *Appl. Organomet. Chem.* 2023, 37, e7108.
16. S. S. Emmanuel, A. A. Adesibikan, *Water Environ. Res.* 2021, 93, 2873–2882.
17. A. A. Bayode, S. S. Emmanuel, A. Osti, C. G. Olorunnisola, A. O. Egbedina, D. T. Koko, D. T. Adedipe, B. Helmreich, M. O. Omorogie, *J. Water Proc. Eng.* 2024, 58, 104753.
18. S. S. Emmanuel, C. O. Olawoyin, A. A. Adesibikan, S. A. Nafiu, A. A. Bayode, *J. Organomet. Chem.* 2024, 1005, 122984.
19. W. S. Koe, J. W. Lee, W. C. Chong, Y. L. Pang, L. C. Sim, *Environ. Sci. Pollut. Res. Int.* 2020, 27, 2522–2565.
20. J. Ni, J. Lei, Z. Wang, L. Huang, H. Zhu, H. Liu, F. Hu, T. Qu, H. Yang, H. Yang, C. Gong, *Nanomaterials* 2023, 13, 142.
21. M. Jamshaid, M. A. Nazir, T. Najam, S. S. A. Shah, H. M. Khan, A. ur Rehman, *Chem. Phys. Lett.* 2022, 805, 139939.
22. P. Veerakumar, A. Sangili, K. Saranya, A. Pandikumar, K. C. Lin, *Chem. Eng. J.* 2021, 410, 128434.
23. R. de Oliveira, W. da Silva Martini, A. C. Sant'Ana, *Environ. Nanotechnology, Monit. Manag.* 2022, 17, 100657.
24. E. M. Hotze, T. Phenrat, G. V. Lowry, *J. Environ. Qual.* 2010, 39, 1909–1924.
25. S. H. Chang, S. B. Lee, D. Y. Jeon, S. J. Park, G. T. Kim, S. M. Yang, S. C. Chae, H. K. Yoo, B. S. Kang, M. J. Lee, T. W. Noh, *Adv. Mater.* 2011, 23, 4063.
26. S. S. Emmanuel, A. A. Adesibikan, C. Olusola Olawoyin, A. A. Bayode, *ChemistrySelect* 2023, 8, e202302712.
27. D. Vaya, P. K. Surolia, *Environ. Technol. Innov.* 2020, 20, 101128.
28. H. H. Shanaah, E. F. H. Alzaimoor, S. Rashdan, A. A. Abdalhafith, A. H. Kamel, *Sustainability* 2023, 15, 7336.
29. F. Ahmad, S. Nisar, M. Mehmood, *J. Chem. Soc. Pak.* 2022, 44.
30. S. H. Khan, B. Pathak, *Environ. Nanotechnology, Monit. Manag.* 2020, 13, 100290.
31. M. Hadei, A. Mesdaghinia, R. Nabizadeh, A. H. Mahvi, S. Rabbani, K. Naddafi, *Environ. Sci. Pollut. Res. Int.* 2021, 28, 13055–13071.
32. U. L. Usman, B. K. Allam, S. Banerjee, N. B. Singh, *Role Green Chem. Ecosyst. Restor. to Achieve Environ. Sustain.* 2024, 301–314.
33. T. Khedr, A. A. Hammad, A. M. Elmarsafy, E. Halawa, M. Soliman, *J. Hazard. Mater.* 2019, 373, 23–28.
34. M. A. El-Sheikh, T. Hadibarata, A. Yuniarto, P. Sathishkumar, E. M. Abdel-Salam, A. A. Alatar, *Chemosphere* 2021, 268, 128873.
35. M. Rani, U. Shanker, V. Jassal, *J. Environ. Manage.* 2017, 190, 208–222.
36. P. Kajitvichyanukul, V.-H. Nguyen, T. Boonupara, L.-A. P. Thi, A. Watcharenwong, S. Sumitsawan, P. Udomkun, *Environ. Res.* 2022, 212, 113336.
37. F. S. Bruckmann, C. Schnorr, L. R. Oviedo, S. Knani, L. F. O. Silva, W. L. Silva, G. L. Dotto, C. R. Bohn Rhoden, *Molecules* 2022, 27, 6261.
38. G. K. Yadav, M. Ahmaruzzaman, *J. Nanopart. Res.* 2021, 23, 213.
39. A. Shamim, K. Neelam, S. Kamaal, A. Ali, M. Ahmad, *Int. J. Environ. Sci. Technol.* 2024, 21, 4653–4684.
40. T. Wu, L. Mao, X. Liu, B. Wang, C. Lin, M. Xin, M. He, W. Ouyang, *Environ. Pollut.* 2021, 290, 118074.

41. J. yi Zhao, Z. xiang Zhan, M. jua Lu, F. biao Tao, D. Wu, H. Gao, *Ecotoxicol. Environ. Saf.* 2022, 243, 113973.
42. P. Montuori, E. De Rosa, F. Di Duca, B. De Simone, S. Scippa, I. Russo, M. Sorrentino, P. Sarnacchiaro, M. Triassi, *Toxics* 2022, 10, 377.
43. W. Zhang, J. Li, Y. Zhang, X. Wu, Z. Zhou, Y. Huang, Y. Zhao, S. Mishra, P. Bhatt, S. Chen, *J. Hazard. Mater.* 2022, 432, 128689.
44. M. A. Hassaan, A. El Nemr, *Egypt. J. Aquat. Res.* 2020, 46, 207–220.
45. R. M. de Souza, D. Seibert, H. B. Quesada, F. de Jesus Bassetti, M. R. Fagundes-Klen, R. Bergamasco, *Process Saf. Environ. Prot.* 2020, 135, 22–37.
46. H. Li, Y. Jiao, L. Li, X. Jiao, *Comp. Biochem. Physiol. Part C* 2023, 271, 109673.
47. J. Zhang, S. Zeng, Y. Liang, L. Qin, H. Zeng, C. Ma, *J. Agro-Environment Sci.* 2021, 40, 2021–0208.
48. G. Zhong, Z. Wu, N. Liu, J. Yin, *Aquat. Toxicol.* 2018, 201, 91–98.
49. M. H. Uddin, M. Shahjahan, A. K. M. Ruhul Amin, M. M. Haque, M. A. Islam, M. E. Azim, *Aquac. Reports* 2016, 3, 88–92.
50. T. O. Ajiboye, A. T. Kuvarega, D. C. Onwudiwe, *Appl. Sci.* 2020, 10, 6286.
51. S. M. Ensley, in Vet. Toxicol., Elsevier, 2018, pp. 509–513.
52. C. A. Schriever, M. Liess, *Sci. Total Environ.* 2007, 384, 264–279.
53. A. O. Adeola, B. A. Abiodun, D. O. Adenuga, P. N. Nomngongo, *J. Contam. Hydrol.* 2022, 248, 104019.
54. S. Yuan, F. Yang, H. Yu, Y. Xie, Y. Guo, W. Yao, *Food Chem.* 2021, 360, 130042.
55. T. L. R. Silva, M. E. L. R. de Queiroz, A. F. de Oliveira, A. A. Z. Rodrigues, A. A. Neves, P. A. F. eira, J. H. de Queiroz, V. O. d. P. Barbosa, *J. Environ. Sci. Heal. - Part B Pestic. Food Contam. Agric. Wastes* 2022, 57, 165–175.
56. B. Y. Fosu-Mensah, E. D. Okoffo, G. Darko, C. Gordon, *Environ. Syst. Res.* 2016, 5, 1–12.
57. L. M. Hu, T. Lin, X. F. Shi, Z. S. Yang, H. J. Wang, G. Zhang, Z. G. Guo, *Geophys. Res. Lett.* 2011, 38, L03602.
58. K. A. Sumon, H. Rashid, E. T. H. M. Peeters, R. H. Bosma, P. J. Van den Brink, *Chemosphere* 2018, 206, 92–100.
59. N. Ali, Kalsoom, S. Khan, Ihsanullah, I. ur Rahman, S. Muhammad, *Expo. Heal.* 2018, 10, 259–272.
60. F. M. Adebiyi, O. T. Ore, A. O. Adeola, S. S. Durodola, O. F. Akeremale, K. O. Olubodun, O. K. Akeremale, *Environ. Chem. Lett.* 2021, 19, 3243–3262.
61. E. Oruc, *Bull. Environ. Contam. Toxicol.* 2012, 88, 678–684.
62. J. Tang, W. Wang, Y. Jiang, W. Chu, *Environ. Pollut.* 2021, 269, 116129.
63. N. Leadprathom, P. Parkpian, J. Satayavivad, R. D. Delaune, A. Jugsujinda, *J. Environ. Sci. Health Part B* 2009, 44, 249–261.
64. O. Akoto, A. A. Azuure, K. D. Adotey, *Springerplus* 2016, 5, 1–11.
65. B. Kumar, S. Kumar, R. Gaur, G. Goel, M. Mishra, S. K. Singh, D. Prakash, C. S. Sharmaa, *Soil Water Res.* 2011, 6, 190–197.
66. J. C. Akan, *J. Environ. Anal. Toxicol.* 2013, 03, 171–178.
67. R. Q. Yang, A. H. Lv, J. B. Shi, G. Bin Jiang, *Chemosphere* 2005, 61, 347–354.
68. B. Li, Y. Hu, Z. Shen, Z. Ji, L. Yao, S. Zhang, Y. Zou, D. Tang, Y. Qing, S. Wang, G. Zhao, X. Wang, **2021**, 947–964.
69. F. Su, P. Li, J. Huang, M. Gu, Z. Liu, Y. Xu, *Sci. Rep.* 2021, 11, 85.
70. V. Usha Vipinachandran, S. Rajendran, K. H. Badagoppam Haroon, I. Ashokan, A. Mondal, S. K. Bhunia, *ACS Appl. Nano Mater.* 2020, 3, 11659–11687.
71. Á. D. J. Ruíz-baltazar, **2020**, *120*, 108158.
72. M. Rani, Keshu, U. Shanker, *Chemosphere* 2024, 352, 141337.

73. F. Hassanzadeh-Afruzi, A. Maleki, E. N. Zare, *Int. J. Biol. Macromol.* 2022, 203, 445–456.
74. S. Batool, A. A. Shah, A. F. Abu Bakar, M. J. Maah, N. K. Abu Bakar, *Chemosphere* 2022, 289, 133011.
75. I. A. W. Tan, A. L. Ahmad, B. H. Hameed, *J. Hazard. Mater.* 2009, 164, 473–482.
76. P. Nalaya, S. A. Wahid, H. E. M. Izuan, *J. Water Environ. Technol.* 2020, 18, 314–326.
77. M. Vithanage, I. Herath, Y. A. Almaroai, A. U. Rajapaksha, L. Huang, J.-K. Sung, S. S. Lee, Y. S. Ok, *Environ. Geochem. Health* 2017, 39, 1409–1420.
78. M. Kah, G. Sigmund, F. Xiao, T. Hofmann, *Water Res.* 2017, 124, 673–692.
79. Z. Wang, L. Han, K. Sun, J. Jin, K. S. Ro, J. A. Libra, X. Liu, B. Xing, *Chemosphere* 2016, 144, 285–291.
80. M. Zhang, Y. Liu, T. Li, W. Xu, B. Zheng, X. Tan, H. Wang, Y. Guo, F. Guo, S. Wang, *RSC Adv.* 2015, 5, 46955–46964.
81. X. Zhu, C. Yuan, Y. Bao, J. Yang, Y. Wu, *J. Mol. Catal. A* 2005, 229, 95–105.
82. S. Vigneshwaran, J. Preethi, S. Meenakshi, *Int. J. Biol. Macromol.* 2019, 132, 289–299.
83. L. Andronic, M. Lelis, A. Enesca, S. Karazhanov, *Surfaces and Interfaces* 2022, 32, 102123.
84. I. S. Grover, S. Singh, B. Pal, *Appl. Surf. Sci.* 2013, 280, 366–372.
85. K. Nagaveni, M. S. Hegde, N. Ravishankar, G. N. Subbanna, G. Madras, *Langmuir* 2004, 20, 2900–2907.
86. J. Huang, S. Wen, J. Liu, G. He, *J. Nat. Gas Chem.* 2012, 21, 302–307.
87. H. Chawla, S. Garg, J. Rohilla, Á. Szamosvölgyi, A. Efremova, I. Szenti, P. P. Ingole, A. Sápi, Z. Kónya, A. Chandra, *J. Cleaner Prod.* 2022, 367, 132923.
88. G. R. M. Echavia, F. Matzusawa, N. Negishi, *Chemosphere* 2009, 76, 595–600.
89. R. Ningthoujam, B. Sahoo, P. Ghosh, A. Shivani, P. Ganguli, S. Chaudhuri, *Nanotechnol. Environ. Eng.* 2023, 8, 581–589.
90. N. Mehrotra, R. M. Tripathi, F. Zafar, M. P. Singh, *IEEE Trans. Nanobioscience* 2017, 16, 280–286.
91. M. Rani, U. Shanker, *Environ. Sci. Pollut. Res. Int.* 2018, 25, 10878–10893.
92. B. Pushkar, P. Sevak, *Int. J. Pharm. Sci. Rev. Res.* 2019, 55, 84–90.
93. M. Rani, Keshu, Ankit, U. Shanker, *ChemistrySelect* 2023, 8, e202300270.
94. T. Wang, J. Lin, Z. Chen, M. Megharaj, R. Naidu, *J. Cleaner Prod.* 2014, 83, 413–419.
95. R. Kumar, N. Singh, S. N. Pandey, *Int. J. Environ. Sci. Technol.* 2015, 12, 3943–3950.
96. W. A. El-Said, D. M. Fouad, M. H. Ali, M. A. El-Gahami, *Int. J. Environ. Sci. Technol.* 2018, 15, 1731–1744.
97. K. M. Paknikar, V. Nagpal, A. V. Pethkar, J. M. Rajwade, *Sci. Technol. Adv. Mater.* 2005, 6, 370–374.
98. S. Choudhary, M. Rani, U. Shanker, *Environ. Nanotechnology, Monit. Manag.* 2022, 18, 100746.
99. A. Iqbal, A. ul Haq, G. A. Cerrón-Calle, S. A. R. Naqvi, P. Westerhoff, S. Garcia-Segura, *Catalysts* 2021, 11, 806.
100. Keshu, M. Rani, U. Shanker, *J. Mol. Liq.* 2023, 387, 122611.
101. P. Phuinthiang, P. Kajitvichyanukul, *Water Sci. Technol.* 2019, 79, 905–910.
102. T. M. S. Rosbero, D. H. Camacho, *J. Environ. Chem. Eng.* 2017, 5, 2524–2532.
103. M. Moustafa, M. A. Abu-Saied, T. Taha, M. Elnouby, M. El-Shafeey, A. G. Alshehri, S. Alamri, A. Shati, S. Alrumman, H. Alghamdii, *Int. J. Biol. Macromol.* 2021, 168, 116–123.
104. S. K. Das, A. R. Das, A. K. Guha, *Langmuir* 2009, 25, 8192–8199.
105. D. Pathania, A. Sharma, S. Kumar, A. K. Srivastava, A. Kumar, L. Singh, *Chemosphere* 2021, 277, 130315.

106. X. Weng, L. Ma, M. Guo, Y. Su, R. Dharmarajan, Z. Chen, *Chem. Eng. J.* 2018, 353, 482–489.
107. J. C. Nnaji, J. F. Amaku, O. K. Amadi, S. I. Nwadinobi, *Sci. Rep.* 2023, 13, 2170.
108. C. Ondijo, F. Kengara, I. K'Owino, *J. Nanobiotechnol.* 2022, 2022, 1–17.
109. D. K. Malik, *Indian J. Chem. Technol.* 2023, 30, 398–402.
110. K. Chinnappa, P. Karuna Ananthai, P. P. Srinivasan, C. Dharmaraj Glorybai, *Environ. Sci. Pollut. Res. Int.* 2022, 29, 58121–58132.
111. J. O. Ighalo, O. J. Ajala, G. Umenweke, S. Ogunniyi, C. A. Adeyanju, C. A. Igwegbe, A. G. Adeniyi, *J. Environ. Chem. Eng.* 2020, 8, 104264.
112. E. M. Alrobayi, A. M. Algubili, A. M. Aljeboree, A. F. Alkaim, F. H. Hussein, *Part. Sci. Technol.* 2017, 35, 14–20.
113. M. Rani, U. Shanker, *Colloids Surf. A* 2018, 559, 136–147.
114. S. M. Mousa, N. S. Ammar, H. A. Ibrahim, *J. Saudi Chem. Soc.* 2016, 20, 357–365.
115. T. A. Devi, R. Jeykumar, R. Ilangovan, *in Lect. Notes Civ. Eng.* 2022.
116. V. Jassal, U. Shanker, B. S. Kaith, S. Shankar, *RSC Adv.* 2015, 5, 26141–26149.
117. V. Jassal, U. Shanker, B. S. Kaith, *Scientifica (Cairo).* 2016, 2016, 1–14.
118. C. O. Ondijo, O. K'owino, F. O. Kengara, in Adv. Phytochem. Text. Renew. Energy Res. Ind. Growth, CRC Press, 2022, pp. 132–135.
119. A. Sharma, K. K. Thakur, P. Mehta, D. Pathania, *Sustain. Chem. Pharm.* 2018, 9, 1–11.
120. P. Pourhakkak, A. Taghizadeh, M. Taghizadeh, M. Ghaedi, S. Haghdoust, *in Interface Sci. Technol.* 2021, 33, 1–70.
121. T. A. Saleh, *in Interface Sci. Technol.* 2022, 34, 39–64.
122. C. T. Umeh, A. B. Akinyele, N. H. Okoye, S. S. Emmanuel, K. O. Iwuozor, I. P. Oyekunle, J. O. Ocheje, J. O. Ighalo, *Environ. Nanotechnology, Monit. Manag.* 2023, 20, 100891.
123. A. A. Bayode, C. Olisah, S. S. Emmanuel, M. O. Adesina, D. T. Koko, *RSC Adv.* 2023, 13, 22675–22697.
124. S. S. Emmanuel, C. O. Olawoyin, A. A. Adesibikan, E. A. Opatola, *J. Polym. Environ.* 2023, 32, 1–30.
125. K. O. Iwuozor, C. T. Umeh, S. S. Emmanuel, E. C. Emenike, A. U. Egbemhenghe, O. T. Ore, T. T. Micheal, F. O. Omoarukhe, P. A. Sagboye, V. E. Ojukwu, *Water Pract. Technol.* 2023, 18, 3065–3108.
126. F. Hassanzadeh-Afruzi, G. Heidari, A. Maleki, *Mater. Chem. Horizons* 2022, 1, 107–122.
127. J. Huang, L. Dou, J. Li, J. Zhong, M. Li, T. Wang, *J. Hazard. Mater.* 2021, 403, 123857.
128. A. V. Baskar, N. Bolan, S. A. Hoang, P. Sooriyakumar, M. Kumar, L. Singh, T. Jasemizad, L. P. Padhye, G. Singh, A. Vinu, *Sci. Total Environ.* 2022, 822, 153555.
129. M. Vakili, S. Deng, G. Cagnetta, W. Wang, P. Meng, D. Liu, G. Yu, *Sep. Purif. Technol.* 2019, 224, 373–387.
130. S. Batool, M. Hasan, M. Dilshad, A. Zafar, T. Tariq, A. Shaheen, R. Iqbal, Z. Ali, T. Munawar, F. Iqbal, S. G. Hassan, X. Shu, G. Caprioli, *Biochem. Syst. Ecol.* 2022, 105, 104535.
131. M. Rani, Keshu, Usha, U. Shanker, *ChemistrySelect* 2023, 8, e202203540.
132. J. O. Ighalo, P. S. Yap, K. O. Iwuozor, C. O. Aniagor, T. Liu, K. Dulta, F. U. Iwuchukwu, S. Rangabhashiyam, *Environ. Res.* 2022, 212, 113123.

133. E. R. Bandala, D. Stanisic, L. Tasic, *Environ. Sci. Water Res. Technol.* 2020, 6, 3195–3213.
134. P. Chellamuthu, F. Tran, K. P. T. Silva, M. S. Chavez, M. Y. El-Naggar, J. Q. Boedicker, *Microb. Biotechnol.* 2019, 12, 161–172.
135. K. O. Iwuozor, S. S. Emmanuel, M. O. Ahmed, A. M. Idris, E. C. Emenike, O. D. Saliu, A. H. Qudus, A. G. Adeniyi, *Chem. Africa* 2023, 7, 539–563.
136. J. O. Oladipo, O. O. Oluwaniyi, S. S. Emmanuel, B. T. Oyewo, G. V. Awolola, S. A. Oyeyinka, O. A. Omole, *Agric. Conspec. Sci.* 2023, 88, 1–6.

Biographical Information

Stephen Sunday Emmanuel received his Bachelor's Degree and Postgraduate Degree in Industrial Chemistry both from the University of Ilorin, Nigeria in 2015 and 2021 respectively. He also earned an MSc. degree in Biotechnology from the Moscow Institute of Physics and Technology. He is currently a Ph.D. scholar at the University of Johannesburg and his research centered around Material Sciences and Environmental Chemistry with a special interest in green synthesis of novel functional materials (nanomaterials, COFs, and MXenes) with applications in energy storage (supercapacitors and batteries), and water pollutants elimination via adsorption and advanced oxidation processes like photocatalytic degradation.

Mustapha Omenesa Idris holds a first-class B.Sc. Industrial Chemistry degree from Bayero University Kano, Nigeria. He proceeded to the University of Benin, Nigeria where he obtained an M.Sc in Industrial Chemistry in 2018. He is currently a Ph.D. scholar at the Universiti Sains Malaysia under the Tertiary Education Trust Fund (TETFund) sponsorship. His current research is focused on anode materials for enhanced microbial fuel cells (MFC) with a major focus on the fabrication of anode materials from biowaste. His focus is to improve energy production and wastewater bioremediation through MFC

Christopher Olusola Olawoyin holds a bachelor's degree in Biochemistry from the University of Ilorin, Nigeria. Presently, he is pursuing his graduate studies in Chemistry and Materials Science at Novosibirsk State University, Russia. He works as a graduate researcher at the Nikolaev Institute of Inorganic Chemistry, SB RAS, where his focus lies in developing synthetic methods for novel molybdenum cluster complexes with promising biomedical applications. Additionally, he is engaged in devising techniques for the fabrication of innovative functional materials from these complexes, emphasizing their properties relevant to biology and medicine, such as radiopacity, luminescence, photosensitivity, and photocatalytic activity.

Ademidun Adeola Adesibikan received her BSc. degree (2015) and MSc. degree (2021) in Industrial Chemistry, both from the University of Ilorin, Nigeria. She is currently undergoing her doctoral study at the University of Pretoria, South Africa as a recipient of the prestigious UP Commonwealth Doctoral Scholarship. Her ongoing research focuses on Material and Environmental Chemistry with her primary goal being able explore the applications of functional materials such as nanomaterials for the removal of water pollutants through adsorption, photocatalytic degradation, and other advanced oxidation processes. Her track record includes co-authored research and review publications indicating a strong collaborative teamwork attitude.

Abdulbasit A. Aliyu obtained his BSc. (2013) from Kogi State (Prince Abubakar Audu) University Anyigba and MSc. (2017) from the University of Ilorin, Nigeria. He is currently a PhD student in Bioinorganic Chemistry in Prof. Joshua Obaleye's research group at the University of Ilorin, Nigeria. In 2023, he was a visiting researcher at the Inorganic and Nano-Materials Research Group at the University of Kwa-Zulu Natal, South Africa. His research focuses on the biological potential of metal-based therapeutics, with particular emphasis on the design and mechanism of action of metal complexes, organometallic anticancer, and anti-inflammatory complexes.

Abdulrahman Itopa Suleiman holds a Bachelor of Science degree (BSc) in Biochemistry from the University of Ilorin, Nigeria in the year 2016. Further to this, He obtained a Master of Science (MSc) degree in Biotechnology with Distinction honors from Bayero University, Kano, Nigeria. His current research involves understanding the role of IL-17 A-targeting microRNA in the mechanism governing cartilage